Precision measurement of the isospin dependence in the 2N and 3N short range correlation region

P. Solvignon (co-spokesperson and contact), D. Higinbotham (co-spokesperson), D. Gaskell
Thomas Jefferson National Accelerator Facility, Newport News, VA 23606

J. Arrington (co-spokesperson), D. F. Geesaman, K. Hafidi, R. Holt, P. Reimer
Argonne National Laboratory, Argonne, IL 60439

D. B. Day (co-spokesperson), H. Baghdasaryan, N. Kalantarians
University of Virginia, Charlottesville, VA, 22901

F. Benmokhtar
Christopher Newport University, Newport News, Virginia, 2360X

A.T. Katramatou and G.G. Petratos
Kent State University, Kent, OH 44242

W. Bertozzi, S. Gilad, V. Sulkosky
Massachusetts Institute of Technology, Cambridge, MA 02139

R. Ransome
Rutgers, the State University of New Jersey, Piscataway, NJ 08854

E. Piasetzky, I. Pomerantz
Tel Aviv University, Tel Aviv, 69978 Israel

G. Ron
The Weizmann Institute of Science, Rehovot, 76100 Israel

E. J. Beise
University of Maryland, College Park, MD 20742

A. Atkins, T. Badman, J. Maxwell, S. Phillips, K. Slifer, R. Zielinski
University of New Hampshire, Durham, NH 03823

N. Fomin
Los Alamos National Laboratory, Los Alamos, NM 87545

J. Annand
University of Glasgow, Glasgow G12 8QQ, Scotland, UK

and

The Hall A Collaboration

Abstract

We propose to perform a precision test of the isospin dependence of two-nucleon short range correlations using mirror nuclei: ^{3}He and ^{3}H. We will also extend the cross section ratio measurement to the $x > 2$ region where three-nucleon short range correlations dominate. This will constitute the first test of the isospin structure of three-nucleon clusters. In parallel to the SRC measurement with the left HRS, we will take data in the quasi-elastic and the resonance regions with the right HRS. The unpolarized electron beam at energies of 2.2 and 4.4 GeV, the under-design room temperature ^{3}He and ^{3}H target system and both high resolution spectrometers (HRS) in standard electron detection configuration are needed for our proposed measurement. The ^{3}H target system passed a first review and the MARATHON experiment (E12-10-103) has been fully approved by PAC37 with an A rating. The proposed measurement requires 19 days of beam time including calibration, overhead, and background measurements.

I. INTRODUCTION TO SHORT RANGE CORRELATIONS

Short-Range correlations (SRCs) have been recognized as responsible for the high momentum tail of the nucleon momentum distribution in nuclei. In the dense enclosure of nuclei, the attractive core produces overlaps between nucleon wavefunctions. The strong short-range repulsive core leads to hard interactions between nucleons that are close together, yielding nucleon pairs which have large relative momenta but a small total momentum, referred to as short-range correlations.

Measurements of the spectroscopic strengths for the nuclear valence orbitals via the (e,e'p) reactions [1] exhibit a 30-40% missing strength compared to the mean field expectation (see Fig. 1). This discrepancy was attributed in part to the hard, short-range repulsive interaction, neglected in the shell model. The hard N–N interaction at short range yields nucleons with high momenta, including a significant contribution with $k > k_F$, the Fermi momentum. This results in strength shifted away from the shells in the single-particle picture and thus the reduction in the spectroscopic strength.

While single nucleon knockout reactions A(e,e'p) allow us to look at the shell model contributions, it is much more difficult to directly probe the high-momentum nucleons generated by correlations, as the cross section in this region is dominated by other processes such as final-state interactions and meson-exchange currents [2–4]. Inclusive electron scattering at $x > 1$ can be used to probe these high-momentum nucleons, providing cleaner measurements that complement the more detailed measurements possible in coincidence reactions.

By choosing the kinematic region where the nucleon momentum is well above the Fermi momentum, the cross section will be dominated by the scattering on high momentum nucleons belonging to short-range correlations. For a free nucleon, the Bjorken variable x ranges from 0 to 1. For nuclei, $x > 1$ implies that more than one nucleon

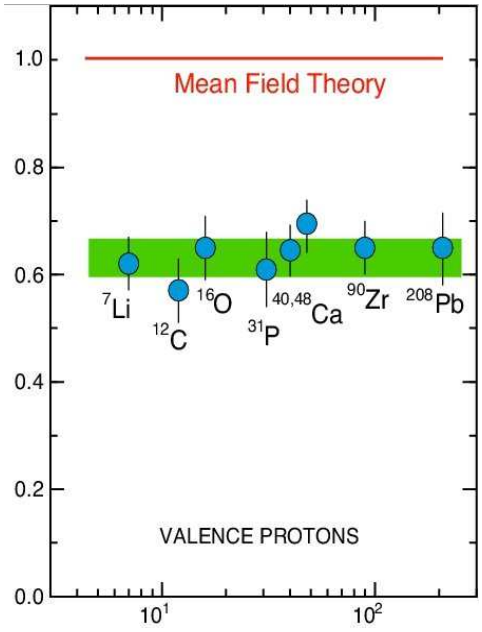

FIG. 1: Quasi-particle strength for valence orbitals. Figure reproduced from [1].

are involved in the scattering. Near $x = 1$, where quasi-elastic scattering dominates the reaction, the contribution of multiple nucleons comes through the mean field interactions which generate the nucleon's Fermi motion which broadens the quasi-elastic peak, extending the strength of the single particle reaction to $x \approx 1.3$. Above this, the scattering is dominated by scattering from a two-nucleon short range correlations (2N-SRC), i.e. a pair of strongly interacting nucleons with large relative momentum but small total momentum. These 2N-SRCs dominate from $x = 1.3$ to $x \approx 2$; above $x = 2$, a nucleon pair with zero total momentum cannot contribute. The strength at $x > 2$ from two-nucleon SRCs (2N-SRCs) arises only because of the net motion of the pair and so falls off very rapidly. Thus, strength significantly above $x = 2$ may similarly be dominated by multi-nucleon clusters, although predictions of the x value where multi-nucleon configurations should dominate is significantly more model dependent, as the place where the 2N contribution becomes negligible depends on the relative momentum distribution of the 2N-SRCs, the total momentum of the SRC, and the strength and x dependence of the 3N-SRC contributions.

Frankfurt and Strikman [5, 6] showed that the cross section for $x \gtrsim 1.3$ (where the single particle contribution is negligible) can be written as a sum of contributions from 2N, 3N,... correlations,

$$\begin{aligned} \sigma_A(x,Q^2) &= \sum_{j=2}^{A} \frac{A}{j} a_j(A) \tilde{\sigma}_j(x,Q^2) \\ &= \frac{A}{2} a_2(A) \tilde{\sigma}_2(x,Q^2) + \frac{A}{3} a_3(A) \tilde{\sigma}_3(x,Q^2) + ..., \end{aligned} \tag{1}$$

where $\tilde{\sigma}_j$ is the cross section for scattering from a j-nucleon correlation. The constants $a_j(A)$ are proportional to the probability of finding a nucleon in a j-nucleon correlation. These constants should fall rapidly with j as nuclei are dilute. In this model, the isospin dependence of the SRCs is neglected (as it is throughout Section I). Taking $a_j(A) = 1$ for $A = j$, i.e. defining $a_2(A)$ to be probability of finding a 2N-SRC in nucleus A relative to deuterium, the cross section σ_j reduces to the cross section for scattering from a nucleus with $A = j$, e.g. for $A = 2$, $\sigma_{eD}(x,Q^2) = a_2(A)\sigma_2(x,Q^2) = \sigma_2(x,Q^2)$, with $\sigma_j(x,Q^2) = 0$ for $x > j$.

In the region where 2N-SRCs dominate, the SRC model predicts scaling of the cross section ratio:

$$(2/A)\sigma_A(x,Q^2)/\sigma_D(x,Q^2) = a_2(A)/a_2(D) = a_2(A), \tag{2}$$

where the factor $(2/A)$ yields the ratio of cross sections per nucleon. Thus, for all values of x and Q^2 where the scattering is dominated by 2N-SRCs, the ratio of the cross section from a heavy nucleus to deuterium (or in fact the ratio of any two nuclei) should be independent of x and Q^2, and be a direct measure of the relative number of 2N-SRCs in the nuclei. While this neglects the effects of FSI, it has been argued [7] that in these small-sized SRCs, the FSI is confined to the nucleons in the correlation itself, and should cancel in the ratio. Similar scaling should be observed in the ratio $A/^3$He in the region where scattering from 3N-SRCs dominates. The SRC model outlined here assumes isospin independence and that the CM of the correlation is at rest.

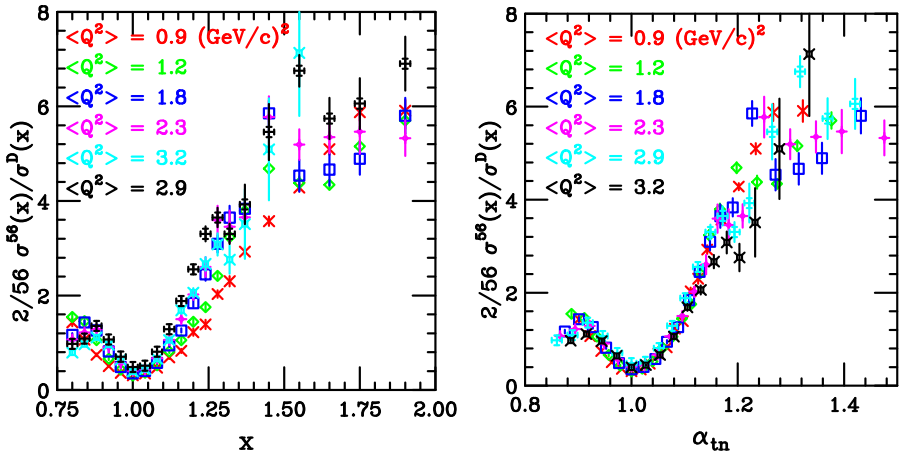

FIG. 2: Evidence of 2N-SRC in the cross section ratio of Fe over deuterium from SLAC data as a function of x and α_{2n} [8] (labeled α_{tn} in the figure).

This scaling behavior for 2N-SRCs was first observed in SLAC data [6, 8]. Figure 2 shows the SLAC results on the cross section ratios of ^{4}He over deuterium at several average Q^2. A plateau can be seen at most of the averaged Q^2 for $x > 1.4$. This is a clear signature of scattering off a strongly correlated pair of nucleons. Scaling seems to get better at high Q^2, as long as the inelastic contribution is still negligible at $x > 1$, but this observation is limited by the statistics. Later measurements in Halls B and C at Jefferson Lab [9–12] made improved measurements providing a more clear plateau and measure of the Q^2 dependence.

We show the data from SLAC in Fig. 2 because it includes both high and low Q^2 values. With this data, it is easy to see the difference between the onset of scaling a function of x and as a function of α_{2n}. The variable α represents the light cone momentum fraction of the struck nucleon [8]:

$$\alpha = A\frac{E_i - p_{i,z}}{E_A - p_{A,z}} = A\frac{E_i^{lab} - p_{i,z}^{lab}}{m_A} \ , \tag{3}$$

where E_i and $p_{i,z}$ are the initial energy and momentum (along the q vector) of the struck nucleon. α is the more appropriate relativistic scaling variable and a cut on α can be used to select nucleons with $k > k_F$, corresponding to the region where mean-field contributions become extremely small. The use of x is an approximation to α and thus the onset of the 2N-SRC dominance, indicated by the plateau, varies in Q^2 while the onset of scaling is Q^2 independent taken as a function of α. However, it is not possible to reconstruct α from inclusive scattering, as it requires knowledge of the initial nucleon momentum and energy. If one assumes that the scattering occurs from a high-momentum nucleon that is part of a 2N-SRC, i.e. that a single nucleon balances the momentum of the struck nucleon, then one can reconstruct α_{2n} from inclusive scattering, which will reproduce the true α to the extent that the 2N-SRC picture is correct. The fact that the transition from the quasielastic peak to the scaling region is essentially

independent of Q^2 when taken as a function of α_{2n} is another indications that the 2N-SRC picture is an accurate representation. We show further results and projections as a function of x rather than α_{2n}, as this is the traditional way to present the data, but note that this yields some Q^2 dependence to the threshold in x where 2N-SRCs dominate. A similar definition is possible in the three-nucleon SRC region, but depends on the assumed distribution of momentum between the nucleons. This will be discussed in more detail when we present the discussion of the structure of the 3N-SRCs.

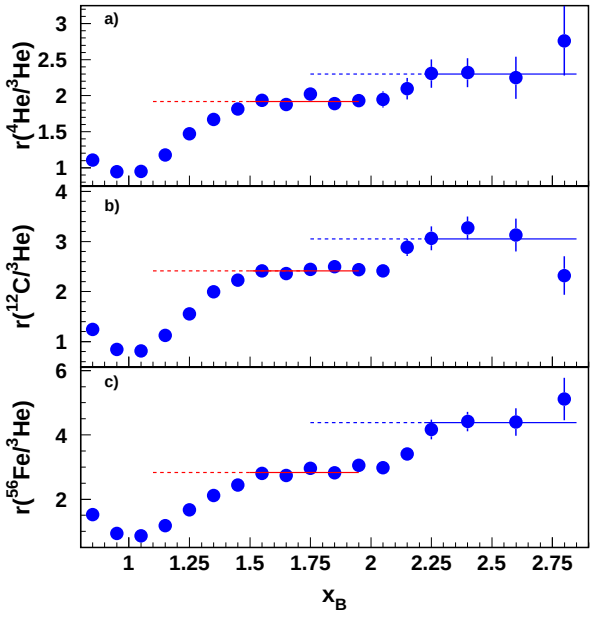

FIG. 3: 2N and 3N correlations from JLab Hall B data [9]. The quantity $r(\mathrm{A}/^3\mathrm{He})$ represent the per-nucleon isoscalar cross section ratios (including a correction for non-isoscalar targets).

In addition to providing higher statistics measurement of the ratios for $1.5 < x < 2$, the results from CLAS [9] (shown in Fig. 3) provided the first indication of scaling in the x-region between 2.25 and 2.80, corresponding to dominance of three-nucleon short range correlations. These data were consistent with the expectation that 3N-SRCs would dominate at sufficiently large x and Q^2, but it was not possible to examine the Q^2 dependence to observe the onset of scaling as there was only sufficient statistics to examine the ratio at low Q^2.

For 2N-SRCs, it is relatively clear where scaling should be observed. Choosing a fixed value of Q^2 and x ($x > 1$) yields a minimum initial struck nucleon momentum as shown in Fig. 4. If that minimum momentum is above the Fermi momentum, then one expects the mean-field contribution to the momentum distribution to be very small and the cross section to be dominated by scattering from 2N-SRCs. However, it is not as clear what initial nucleon momentum will be sufficient for 3N-SRCs to dominate the scattering. The limited data at higher Q^2 [9] showed some suggestion of a possible increase in the ratio with increasing Q^2 [13]. New results from JLab Hall C experiment E02-019 [11] are in good agreement with CLAS in the 2N-SRC region, but yield a significantly higher ratio for $x > 2$, as shown in Fig. 5. E02-019 is at higher Q^2 than CLAS data, and this behavior is consistent with the hint of possible Q^2 dependence in the CLAS results. Experiment E08-014 [13] took high precision data, especially at somewhat larger Q^2, in April-May 2011 and is being analyzed to precisely determine 3N-SRC probabilities $a_3(\mathrm{A}/^3\mathrm{He})$ and to clarify its Q^2 and x dependence.

All the above assumed isospin symmetry in the correlation structure. Recent two-nucleon knockout measure-

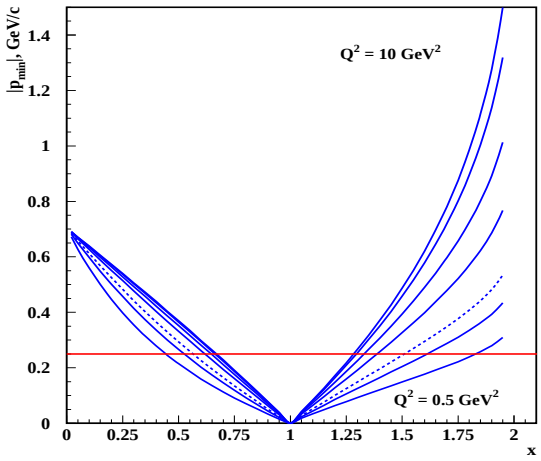

FIG. 4: Minimum momentum of the struck nucleon for quasielastic scattering from a nucleon in a 2N SRC as a function of x for Q^2 values from 0.5 to 10 GeV^2.

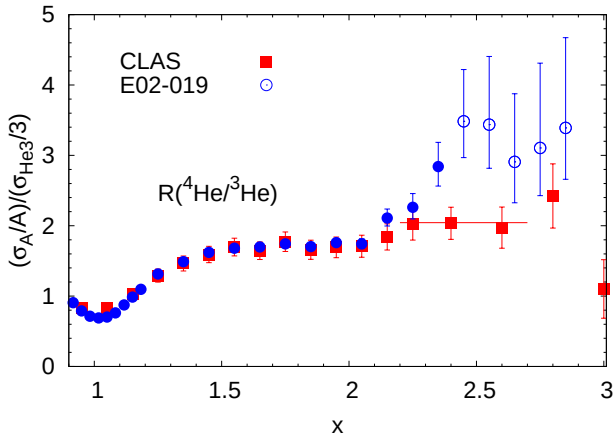

FIG. 5: Cross section ratio (^{4}He/^{3}He) from Hall C experiment E02-019 [11] compared to the CLAS data [9] (no isoscalar correction applied in this extraction). In the $x > 2.25$, the CLAS data have an average $Q^2 \approx 1.6$ GeV^2 while the E02-019 are at much higher averaged Q^2 of about 2.9 GeV^2. The error bars shown for $x \geq 2.4$ (hollow points) represent the central 68% confidence level region.

ments [14, 15] suggest a large difference in the high-momentum contributions coming from "pp" and "pn" pairs. The primary goal of the proposed measurements is to make a more precise, quantitative extraction of the ratio in the 2N-SRC region, although the data will also be able to address other questions related to the structure of SRCs and the reaction mechanism in these inclusive measurements.

II. OVERVIEW OF THE PHYSICS GOALS OF THE EXPERIMENT

We propose to measure inclusive scattering from ^{2}H, ^{3}H, and ^{3}He at large x. The primary goal is to examine the isospin structure of the 2N-SRCs, but these data can also be used to answer other questions about SRCs and test the assumptions that go into the traditional analysis of the inclusive measurements. Ratios of ^{3}He/^{2}H and ^{3}H/^{2}H for $1.5 < x < 2$ will allow for tests of detailed few body calculations, as well as providing information on the A

dependence of 2N-SRCs in light nuclei without the uncertainty associated with the isospin structure of the 2N-SRCs. Comparisons of ^{3}H to ^{3}He for $1.5 < x < 2$ will allow for a measure of the isospin structure of the 2N-SRCs without the presence of the large final-state interactions present in the two-nucleon knockout measurements. Finally, the absolute cross sections for $x > 2$ will provide information on the structure of the 3N-SRCs. These topics are detailed in the following sections.

A. Tests of few-body calculations and final-state interactions

Using the inclusive cross section ratios to extract the contribution of SRCs relies on the assumption that final-state interactions (FSIs) at $x > 1$ and high Q^2 only occur between nucleons that are extremely close together, i.e. are within the SRC being probed [7, 8]. If this is the case, then while there may be non-negligible FSI contributions, they should only come from the 2N-SRCs which have essentially identical structure in all nuclei. Thus, the ratios can be reliably used for extracting the relative contribution of 2N-SRCs. While some calculations such as the Correlated Glauber Approximation (CGA) [16] suggest that this is not the case, and that there are significant FSI contributions that are unrelated to the SRCs even at high Q^2, this is refuted by more recent calculations within the Generalized Eikonal Approximation (GEA) [2, 17]. It has been suggested [18] that the difference is due to the fact that the Glauber approximation, where only elastic rescatterings are accounted for, does not satisfy the unitarity condition and thus the CGA significantly overestimates the FSI contribution to the inclusive cross section. The unitarity condition is automatically accounted for in GEA in which FSI contribution to inclusive cross section is calculated through the imaginary part of the forward virtual Compton scattering off the nuclei [19].

Presently such calculations (with inclusion of SRC effects) are possible only for ^{2}H, ^{3}H, and ^{3}He [18]. Calculations for ^{4}He are significantly more difficult, and while data are available for ^{2}H and ^{3}He, comparison of the calculation to ^{3}He are sensitive to both the details of the FSI in addition to the isospin structure of the SRCs and the relative contribution of the neutron and proton to the inclusive cross section. By measuring both ^{3}H and ^{3}He, one can separate the isospin dependence and the FSI contributions. By comparing to both deuterium and $A = 3$ nuclei, one can directly check for any A dependence in the FSI, which does not occur in the GEA calculation. This will provide crucial information about the role of the FSI at $x > 1$ and large Q^2 that otherwise will be impossible to obtain. The confirmation of the localization of FSI within 2N SRC in these kinematics will have important impact in interpretation of the inclusive $x > 1$ data for medium to heavy nuclei.

B. A dependence of SRCs

Recent Jefferson Lab measurements have provided improved measurements of the A dependence of the SRC contributions in both light and heavy nuclei [11]. Additional corrections, accounting for our present understanding of the isospin structure of the pairs and the fact that the total momentum of the pair is small but non-zero, have also been applied.

For nuclei that are far from $N = Z$, e.g. ^{3}He and ^{197}Au, the assumption made about the isospin structure of the 2N-SRCs has a significant impact ($\lesssim$15%) on the extracted SRC contribution and which also modifies the A dependence since one goes from a large proton excess in ^{3}He to a neutron excess that grows with mass for medium to heavy nuclei. Figure 6 shows the observed A dependence from E02-019, which extracts the relative 2N-SRC contribution, R_{2N} from the ratio of the cross section per nucleon without applying an isoscalar correction as previous measurements have done (solid red circles), and including this correction (hollow cyan circles).

The largest change is in ^{3}He, which is one of the few nuclei available where detailed *ab initio* calculations can be performed. Thus, a careful comparison of the extracted SRC contribution to detailed calculations in ^{3}He and ^{4}He

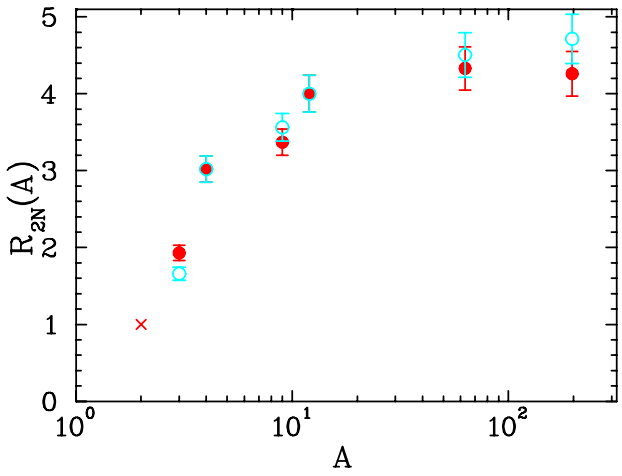

FIG. 6: Extracted contribution of SRCs in nuclei relative to ^{2}H from Ref. [11]. $R_{2N}(A)$ is the probability for a nucleon to be part of a high relative momentum pair with a low total momentum, i.e. a 2N-SRC, relative to the deuteron. It is taken from the cross section ratio in the plateau region with corrections applied for inelastic contributions and the impact of the smearing of the distribution due to the small total momentum of the pair. The solid red points are the result including no correction for non-isoscalar targets, while the hollow cyan points include an isoscalar correction (as applied in extractions prior to Ref. [11].)

including final-state interactions and other effects is extremely important. Such a comparison will be helped if the question of the isospin structure of the high-momentum tails can be separated. This can be accomplished by making measurements of both ^{3}H/^{2}H and ^{3}He/^{2}H, which will be provided by the proposed measurements. One can simply average these results to compare to an isoscalar $A = 3$ calculation, or compare to detailed calculations of both the ^{3}H and ^{3}He ratios.

C. Isospin dependence of SRC

In the SRC model [5, 6], the nucleon correlations are assumed to be isospin independent, with nn, np, and pp pairs all equally likely to yield high-momentum configurations. However recent results from the Hall A two-nucleon knockout experiment E01-015 [14, 20] suggested that the correlated pairs were dominated by np, and that both pp and nn correlations together accounted for only 10% of the total SRCs measured, as shown on Fig. 7. They also find that np pairs have roughly 20 times the contribution of pp pairs in generating extremely high momentum nucleons.

Recent calculations [21, 22] show that for 2N-SRCs at rest in a nucleus, the tensor force yields an excess of high-momentum nucleons in deuteron-like (T=0) np correlations, while nn, pp, np pairs with T=1 are all strongly suppressed. A calculation for several light nuclei is shown in Fig. 8. This clearly demonstrates the dominance of the tensor part in the momentum range 1.4-4.0 fm^{-1} where the correlated pairs are expected to dominate the nuclear wave function.

Experiment E01-015 is kinematically complete and can therefore determine the approximate region of the momentum distribution being probed, within the impulse approximation. The experiment involves measuring $^{12}C(e, e'p)$ at large missing momentum and then using a large acceptance detector to look for nucleon with momenta nearly opposite to the proton's reconstructed initial momentum. The measurement is taken at $x > 1$ to reduce final-state interactions, but these are still extremely large at high values of missing momentum. Thus, the isospin extraction from the triple-coincidence measurement relies on the idea that at $x > 1$ ($x \approx 1.2$ in this case), the FSI may be very large, but only come from rescattering between the struck nucleon and the other nucleon in the SRC, rather than a lower

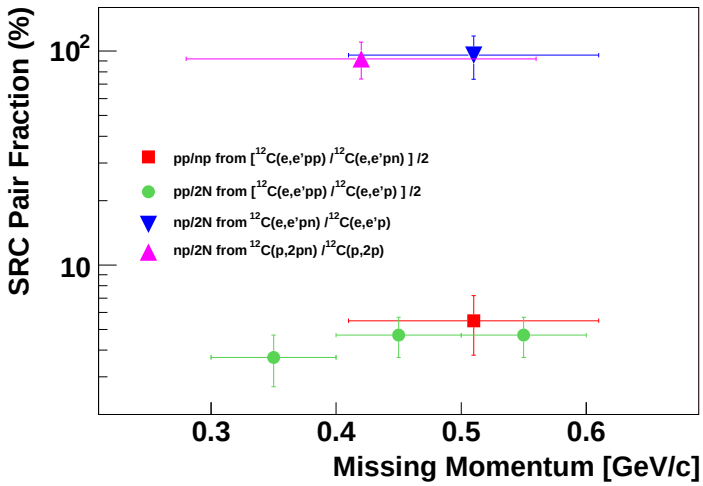

FIG. 7: Results from [15] showing the dominance of np pairs in 2N-SRCs where a proton at high missing momentum is measured and a large acceptance detector looks for a high momentum backwards recoil nucleon.

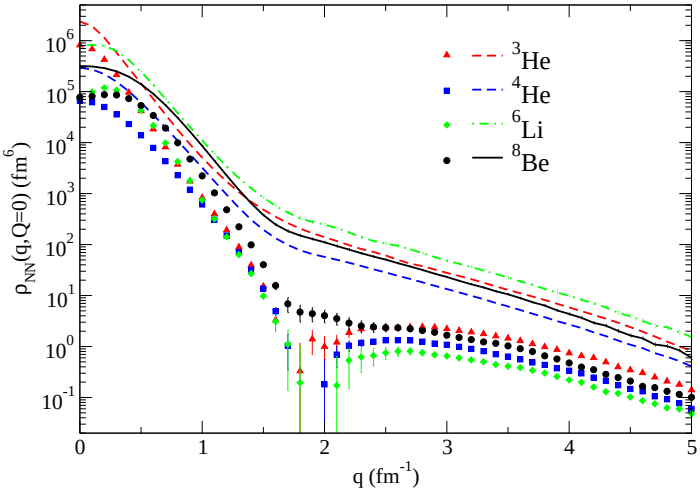

FIG. 8: Calculations of the np and pp relative momentum for pairs with zero total momentum from [21]. The lines represent the np pair relative momentum distribution and the symbols the pp pair relative momentum distribution obtained with fully realistic Av18/UIX hamiltonian. The minimum near $q = 2$ fm^{-1} is essentially the same feature as seen in the S-wave component of the deuteron distribution, while the D-wave contributions fill in the minimum.

momentum nucleon being rescattered to high missing momentum. It is not clear *a priori* that this would be true to a sufficient level that one could interpret the triple-coincidence measurements cleanly. However, any FSI contribution coming from a lower initial missing momentum would tend to yield high-momentum protons and neutrons after the rescattering, and thus only dilute the large asymmetry between np and pp contributions. Nonetheless, FSI corrections must be accounted for in the analysis, including absorption of the nucleon as it exits the nucleus and, in particular, charge-exchange FSI contributions which can modify the isospin of the observed nucleons.

In inclusive measurements, final state interactions at high Q^2 are significantly smaller and any remaining FSIs should cancel in the ratios as they will be similar for 2N-SRCs in all nuclei. However, the inclusive measurement sums over scattering from protons and neutrons and thus provides no information on the isospin structure of the 2N-SRC. By choosing non-isoscalar targets, it is possible to modify the potential contribution from nn, pn, and pp pairs,

and thus test predictions of different models of the isospin structure of SRCs. Thus, this is complementary to the triple-coincidence measurements which can provide more information, but must deal with larger FSI contributions.

While the ratios shown in Fig. 3 are corrected for the difference between the electron-proton and electron-neutron cross sections, they assume that the ratio of neutrons to protons in the 2N-SRCs and 3N-SRCs is equal to the N/Z ratio of the nucleus. We can study these effects using inclusive scattering in the 2N-SRC (or 3N-SRC) dominated regions for nuclei with different N/Z ratios. Detailed calculations exist for few-body nuclei, and it is easy to see the impact of the isospin dependence for the simplest case; the comparison of ^{3}He and ^{3}H. For isospin-independent 2N-SRCs, ^{3}He will have two pn pairs and one pp pair, compared to two pn pairs and one nn pair for ^{3}H. For ^{3}He, this yields four options for a high-momentum proton and two for a high-momentum neutron, yielding a proton distribution that is twice the neutron distribution at large momenta. For ^{3}H, the opposite happens, but in both cases, the ratio of the proton to neutron momentum distributions, $n_p(k)/n_n(k)$ at high momentum is just equal to the Z/N ratio. If deuteron-like SRCs dominate, then each nucleus has two pn pairs and negligible contributions from pp or nn pairs, yielding $n_p(k)/n_n(k) = 1$ for $k > k_F$. So for dominance of T=0 pairs, the cross sections in ^{3}He and ^{3}H at $x \gtrsim 1.5$ will be identical, while for the isospin-independent case, the ratio will be $(2\sigma_p + \sigma_n)/(\sigma_p + 2\sigma_n) \approx 1.4$ for kinematics of the proposal, which yield $\sigma_p \approx 3\sigma_n$.

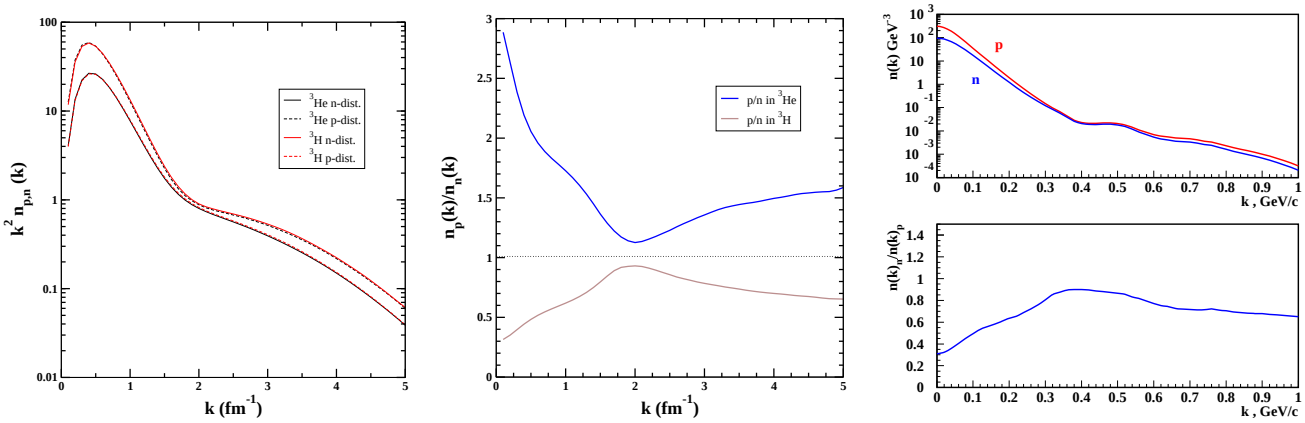

FIG. 9: Left: Momentum distribution for protons (dashed) and neutrons (solid) in ^{3}He (red) and in ^{3}H (black) from Quantum Monte Carlo calculation [23, 24]. Middle: Ratio of proton to neutron distributions from the same calculation. Right: momentum distribution and ratio for ^{3}He from calculation of M. Sargsian [18].

We can also see the impact of the isospin structure of the correlations in the calculated momentum distributions for the proton and neutron in ^{3}He and ^{3}H. The left and central panels of Fig. 9 shows a calculation of the momentum distribution for protons and neutrons in ^{3}He and ^{3}H, as well as their ratio [23, 24], using the Argonne v18 + Urbana IX two-nucleon and three-nucleon potentials. The right panel shows an independent calculation of the same quantities [18]. For the isospin-independent case, the proton-to-neutron ratio would always be Z/N, i.e 2 for ^{3}He and 1/2 in ^{3}H. In the case of dominance of the T=0 np pairs, the ratio in the 2N-SRC dominance region ($k_F < k <$500 MeV/c corresponding to $1.5 < k < 2.5$ fm^{-1} on Fig. 9) would equal 1 in both nuclei. The calculation predicts that the neutron-to-proton ratio at high momenta, where 2N-SRCs dominate, is between 0.5 and 1.0 for ^{3}He. This suggests a significant excess of np pairs over what one would expect from isospin-independent interactions, but not a total dominance of the T=0 pairs, with very similar results coming from the calculation of Ref. [18] (right panel of Fig. 9. The T=0 pair dominance is also obvious in Fig. 10 where pn, pp and nn distributions are plotted versus the relative momentum k for a total pair momentum equal to zero, which corresponds to the two nucleons of the pair moving back to back.

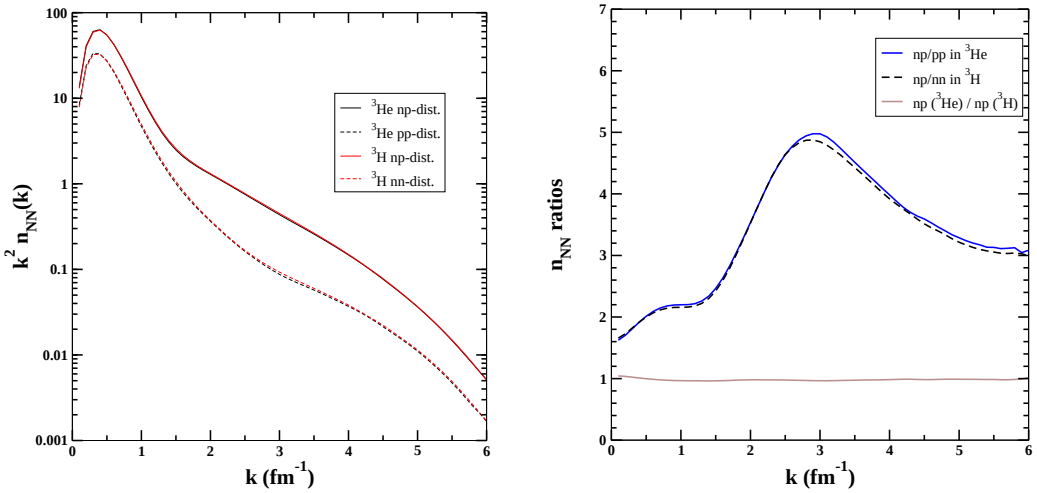

FIG. 10: Left: Momentum distribution of the nucleon np-pair (solid) and nn or pp (dashed) in ^{3}He (black) and ^{3}H (red) as a function of the relative momentum between the two nucleons from Quantum Monte Carlo calculation [23, 24]. Right: Ratio of pn to pp (or nn) distributions. Also plotted is the ratio of the pn distribution in ^{3}He to pn distribution in ^{3}H.

A calculation from M. Sargsian [18] was performed at the lowest Q^2 of our proposed experiment using the Av18/UIX 2N and 3N potentials. This calculation confirms that the 2N-SRC are strongly isospin-dependent and that the scaling regime is reached at $Q^2 \sim 1.5$ (GeV/c)^2. Previous measurements of A/^{2}H cross section ratios at similar kinematics also show a clear plateau for $x > 1.4$ at $Q^2 \sim 1.5$ GeV^2.

the isospin dependence on light mirror nuclei. The 40% difference between $T = 0$ dominance and the isospin-independent case allows an unambiguous distinction between the two assumptions and a clean measure of the ratio $(T = 1)/(T = 0)$. For light nuclei, sophisticated calculations exist and can be compared to our results. The motion of the pair and final state interactions should mostly cancel in the ratio allowing a clean interpretation of our data.

D. Sensitivity to 3N-SRCs

The cross section from ^{3}H and ^{3}He can also be compared at $x > 2$, where 3N-SRCs are expected to have a significant contribution. In this case, there is no question as to the isospins of the nucleons in the 3N-SRC. However, both the absolute cross section and the ratios can provide information on the microscopic structure of the 3N-SRCs, illustrated in Fig. 11.

The scaling in the 2N-SRC region is significantly less Q^2 dependent when taken as a function of α_{2n} rather than x, as shown in Fig. 2. The variable α_{2n} is an approximation to the light cone momentum fraction, calculated by assuming that the struck nucleon is accompanied by a spectator nucleon with equal-but-opposite momentum. The equivalent variable for 3N-SRCs depends on the momentum sharing of the nucleons in the 3N-SRC. If we strike nucleon 3 in the configurations shown in Fig. 11, the spectator system will always have momentum that balances the struck nucleon, but the excitation of the residual system will be larger in configuration (b). Examining the onset of the plateau for the variables derived from assuming these two different configurations should provide some indication as to the dominant configuration. More importantly, these will predict different distributions for the highest momentum nucleons, which can be compared to the absolute cross sections for $x > 2$ on ^{3}He and ^{3}H, where detailed calculations, including final-state interactions, can be performed for both ^{3}H, ^{3}He. The average of the ^{3}H and ^{3}He cross sections, representing an 'isoscalar' A=3 nucleus, can be compared to calculations which to not explicitly include isospin structure.

In addition, information about the isospin configuration can be extracted from these comparisons. In the fully

symmetric configuration shown as Fig. 11(b), the only difference between ^{3}H and ^{3}He will be the total number of protons and neutrons, and the cross section ratio of ^{3}He to ^{3}H will go as $(2\sigma_p + \sigma_n)/(\sigma_p + 2\sigma_n) \approx 1.4$ wherever 3N-SRC contributions dominate. The configuration shown in Fig. 11(a) yields a large asymmetry in the momentum of the nucleons. If the nucleon with the largest momentum, nucleon 3, tends to be the single nucleon, then the ratio of ^{3}He/^{3}H in scattering will be $\sigma_n/\sigma_p \approx 0.35$. If the highest momentum nucleon tends to be one of the doubly occurring nucleons, the the ratio will be approximately $\sigma_p/\sigma_n \approx 3$, while an isospin-insensitive distribution will again yield $(2\sigma_p + \sigma_n)/(\sigma_p + 2\sigma_n) \approx 1.4$.

In any of these cases, the transition from the ratio in the 2N-SRC region (measured in the experiment and expected to be unity in the case of dominance by iso-scalar 2N-SRCs) to the ratio at $x > 2$ will provide a measure of the contribution of 3N-SRCs relative to 2N-SRCs, and help identify the transition from 2N-SRC to 3N-SRC dominance.

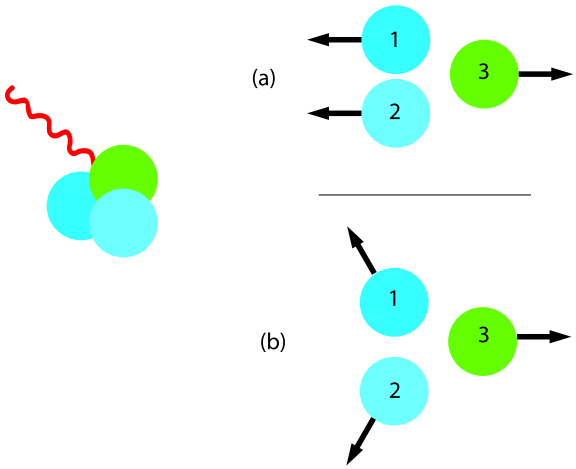

FIG. 11: Illustration of possible "limiting case" 3N-SRC configurations. Note that in configuration (a), the momentum of nucleon 3 is taken to be twice that of nucleons 1 and 2.

III. THE PROPOSED MEASUREMENT

Determining the isospin dependence of the short-range correlation pairs and 3N is an important step in the understanding of the strong force at short distances. In order to access the isospin information, we need to choose kinematics in 2N and 3N-SRC regions where scaling has been established. One of the goals of experiment E08-014 [13] is to determine at which Q^2 the cross section ratios at $x > 2.2$ exhibit scaling. In the present proposal, using the results from SLAC and JLab, we anticipate that measurements of $\sim$1.4 (GeV/c)^2 will allow for a clean extraction of the 2N-SRC contributions. We propose to perform precision measurements of the inclusive electron scattering cross sections for ^{3}H, ^{3}He and ^{2}H with an incident beam energy of 4.4 GeV and with the left HRS at two scattering angles: 17° and 19°. With ^{2}H, ^{3}H and ^{3}He data taken at the same kinematics, one can extract the 2N-SRC ratios $\sigma_A/\sigma_{^2H}$ for both ^{3}H and ^{3}He, as well as taking the average ratio to extract the iso-scalar SRC ratio for A=3. While the 3N-SRC region may not be high enough in Q^2 to cleanly isolate 3N-SRCs, one can perform detailed calculations including FSI and other contributions for these nuclei. In addition, one would also expect contributions from such effects to be very similar in these mirror nuclei, and thus these should be more reliable than ratios of heavier nuclei to ^{3}He. Finally, the 2N-SRC contributions should become negligible at smaller x values for A=3 than in heavier nuclei, as the total momentum of the 2N-SRC pair, which leads to the contributions beyond $x = 2$, should be smaller in the very light

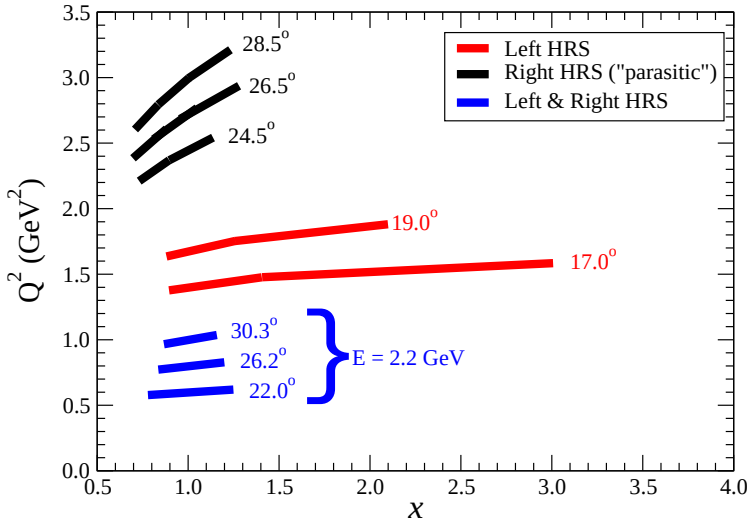

FIG. 12: Kinematic coverage of the proposed experiment. The right HRS "parasitic" kinematics (in black) will be taken in parallel to the SRC measurement (in red), which is the main goal of the experiment.

nuclei.

Taking deuterium data will allow us to directly access spectral functions in the isospin 0 and isospin 1 channels [25]. One can also take the direct ratios of ^{3}H to ^{3}He, which can be compared to the expectations of the different models for the isospin structure of the 2N-SRCs (and 3N-SRCs). In addition, one can form the following ratios:

$$\frac{\left[\sigma(^3He) - \sigma(^3H)\right] / \left[\sigma(^3He) + \sigma(^3H)\right]}{\sigma(^2H)}, \tag{4}$$

which directly measures the spectral function of the isospin 1 correlations, and:

$$\frac{\sigma(^3He) - \sigma(^3H)}{\sigma(^2H)}, \tag{5}$$

which directly measures the difference of the spectral functions in I=1 and I=0 channels. Hence, these results will provide, in an independent way, a test of the observation of the small values of the (e,e'pp)/(e,e'pn) ratios.

Our primary focus is on the $x > 1.3$ region where we can examine the 2N- and 3N-SRC plateaus. Fig 12 shows the x and Q^2 coverage of the proposed experiment. All of the data for $x > 1.3$ is taken with the left HRS, as the maximum momentum limit of 3.2 GeV/c for the right HRS does not allow for measurements in the SRC region. We are proposing to use the right HRS to perform measurements the ^{3}H, ^{3}He and ^{2}H cross sections in the quasi-elastic scattering region over a large Q^2-range of 0.6-3.0 GeV^2. At present, the world data for quasi-elastic scattering on ^{3}H has only reached 0.8 (GeV/c)^2 (at the quasi-elastic peak) as shown in Fig. 13. The low-x side of the QE peak at high Q^2 will extend far enough down to connect to the MARATHON measurement, so that there will be structure function data going from the DIS into the resonance and quasielastic region.

In addition, one day is allocated to running at 2.2 GeV for checkout and low Q^2 comparisons of the QE peak in ^{3}H and ^{3}He. This will allow for an extraction of the neutron magnetic form factor, $G_M^n(Q^2)$, in the region where the QE peak is easy to isolate and where discrepancies exist between world data. The comparison of the QE peak will be dominated by the systematic uncertainties, discussed in Table IV. These uncertainties will be magnified in going from ^{3}H/^{3}He to σ_n/σ_p, yielding an uncertainty of 6%, and an extracted G_M^n value of 3%. We have three low Q^2 points, in the region where there is a discrepancy of ~8% between the measurements from JLab ("CLAS" and "Anderson" in Fig. 14) and comparisons of proton and neutron knockout from the deuteron ("Anklin" in Fig. 14). We can provide

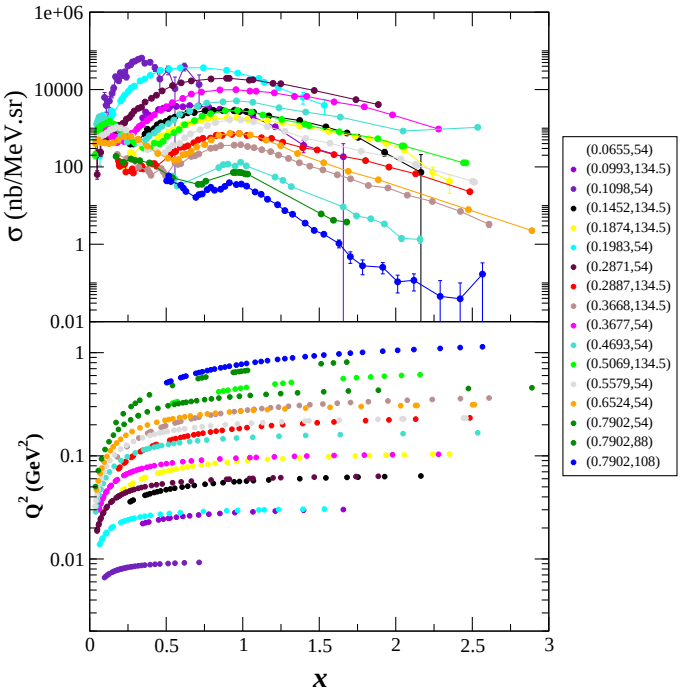

FIG. 13: Existing world data on quasi-elastic scattering off ^{3}H [26]. The legend corresponds to: (incident beam energy in GeV, scattering angle in degree).

measurements with 3% uncertainty at Q^2=0.6, 0.8, and 1.0 GeV^2, bridging the range between the JLab polarization and cross section ratio measurements. Both of these extractions indicate $G_M^n/(\mu_n G_D) < 1$ for $Q^2 < 1$, while the Anklin data yields values of G_M^n that are 8% higher.

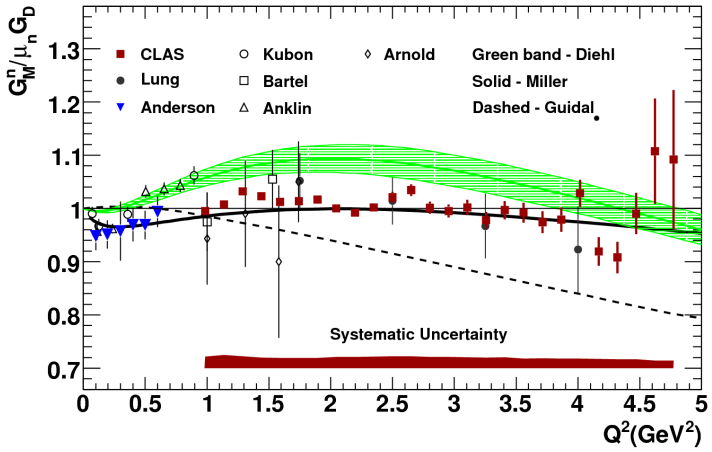

FIG. 14: World's data on G_M^n from Ref. [27]

A. The targets

The ^{3}He and ^{3}H target system was reviewed on June 3, 2010 and the review committee expressed many suggestions but "no-show stoppers" were found. As a result, the MARATHON experiment [28] has been fully approved with an A rating by PAC38 for the measurement of the ^{3}He and ^{3}H ratio in deep inelastic scattering.

To lower the ^{3}H activity, the updated design will have ^{3}He, ^{3}H, ^{2}H and ^{1}H gases, contained in identical 30-cm long aluminum cells at room temperature. The density under consideration for the tritium target is 2.5 mg/cm^3 which corresponds to 1000 Ci. The target system will consist of four identical cells as the one shown in Fig. 15. The tritium cell will have a pressure of 10 atm while the ^{3}He, ^{2}H and ^{1}H cells will be at 20 atm. The diameter of the cell will be 1.25 cm. The windows and walls are required to be thick and the present design assumes a thickness of 18 mils.

More about the safety requirements can be found in Ref. [29].

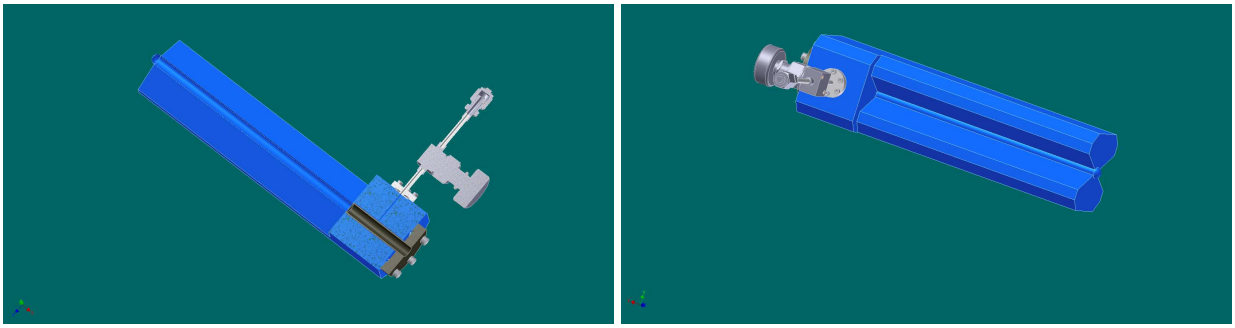

FIG. 15: Latest target design (D. Meekins)

B. Background

1. *Window contributions to the cross section*

From online results of E08-014 which used a 20 cm aluminum cell with window and wall thicknesses of 12 mils, less than 3% window contamination in the 3N-SRC region remains after a software cut on the target variable y_{tg}, as shown on Fig 16. Taking the central ± 3 cm in y_{tg}, corresponding to the central $\sim$15 cm of the target length in z, the endcap contributions are below 3% of the hydrogen yield. This can be reduced further if necessary by cutting out slightly more than the 5 cm (2.5 cm on each end) removed by this cut.

The lower target density and thicker windows ($\sim$18 mils) being considered for the tritium target system would create a larger contamination then observed in E08-014, but the cells are much longer (30 cm) than for E08-014. Therefore the aluminum contamination should be relatively small. To estimate the physics rates of this proposal, we use a tight cut on the target length of $y_{tg} = \pm$ 3.0. This cut on the target length yields an effective target length of 20.5 cm at 17.0°, and will remove significantly larger amount of data near the window then the in E08-014 (which used the central 15 cm of a 20 cm cell), thus increasing the suppression of the endcap contributions. We will take data on a dummy target and use this to estimate and subtract the small residual background contribution left after applying the y_{tg} cut.

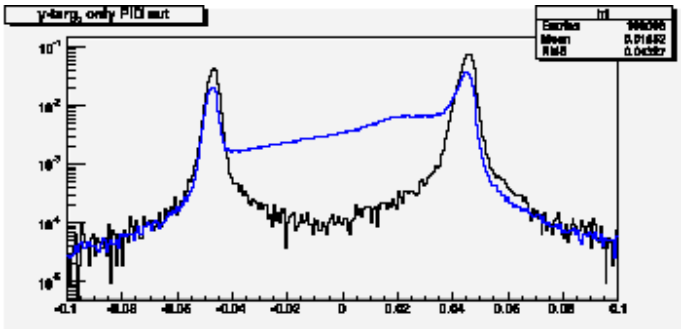

FIG. 16: Y-target spectrum showing the window contribution to the ^{3}He cross section for the 20 cm, high-pressure ^{3}He gas cells used in E08-014. The dummy spectrum is shown in black and the ^{3}He target spectrum in blue, with the spectra normalized to yield the same number of counts.

2. *Pion contamination and charge-symmetric background*

The expected pion background has been evaluated using experimental data of JLab Experiment E89-008 [12]. For an incident energy of 4.045 GeV and at a scattering angle of 23°, the π/e ratio was found to be approximately 10:1 for a 2% RL carbon target at a momentum setting of 3.76 GeV and 4:1 for a 2% RL iron target at 3.60 GeV.

The PID performance of Hall A HRS detectors has been shown to be very good in past experiments (see [30, 31], for example) allowing a reduction of the pion background by a factor of about 10^4, while keeping an electron efficiency better than 99%, when a CO_2 gas Čerenkov counter and double-layer lead glass calorimeter are associated. This yields a worst-case pion contamination of ≈0.1%. Results from the recently completed E08-014 experiment, with data taken under very similar conditions, show that the pion rejection is more than sufficient to remove the background.

The charge-symmetric background can be very large for large scattering angles, but decreases rapidly at smaller angles. For E02-019 [32], the charge-symmetric background for even the high-Z, 6% radiation length targets was always well below 1% for angles below 30° and relatively large values of x ($x \gtrsim 0.6$). For the targets proposed here and scattering angles below 25°, we expect a maximum charge-symmetric background to be below 0.1%.

C. Proposed runplan

To estimate the coverage and the precision of the proposed measurements, a conservative momentum bite of ±3.5% was used. This is sufficient to fully cover the 3N-SRC region in one setting, although using the full HRS momentum acceptance will improve the overlap between settings and range of the QE peak in the acceptance. For extracting the uncertainties, the projected results in x with a binsize of 0.1. The rates for ^{3}He were evaluated using a model based on the data of Ref. [32] on y-scaling for the large x region. This model ("XEM model") was fitted to data on a variety of light and heavy nuclear targets for both the DIS and $x > 1$ region, but with a beam energy of 5.8 GeV.

The angular acceptance $\Delta\Omega$ was estimated at 3.2msr to maintain good acceptance for long target, with a conservative momentum bite ΔP of ±3.5% and an effective target length corresponding to a y_{target} cut of ±3.0cm were chosen to evaluate the physics rates. This cut on the target length yields an effective target length of 20.5 cm at 17.0° and 18.4 cm at 19°. The estimated time needed at each kinematic setting is given in Table I and Table III, as well as the beam currents (I), the total rates (R_{tot}) after prescaling by the factor psc (also listed) and the physics rates (R_{phys}). The rate estimates include acceptance, efficiencies and radiative corrections, and were validated against the observed rates for ^{3}He in E08-014. Table II provides a summary of the required overhead time.

E (GeV)	θ (deg)	E' (GeV)	x_{range}	Q^2_{range} (GeV/c)^2	Tg	I (μA)	psc	R_{tot} (Hz)	R_{phys} (Hz)	time (hrs)	Total (hrs)
4.400	17.0	3.980	1.41-3.00	1.48-1.58	^{3}He	25	1	1181	2.1	75.0	
					^{3}H	25	1	1173	11.5	100.0	**175.0**
4.400	17.0	3.710	0.90-1.41	1.38-1.48	^{3}He	25	5	2880	41	6.0	
					^{3}H	25	5	2840	32	8.0	
					^{2}H	25	5	2909	49	13.0	**27.0**
4.400	19.0	3.790	1.26-2.10	1.75-1.88	^{3}He	25	1	772	2.0	30.0	
					^{3}H	25	1	765	1.5	40.0	
					^{2}H	25	1	773	1.7	87.4	**157.4**
4.400	19.0	3.535	0.88-1.26	1.64-1.75	^{3}He	25	2	2818	42	5.0	
					^{3}H	25	2	2777	33	6.6	
					^{2}H	25	2	2857	51	8.6	**20.2**
2.200	22.0	1.870	0.78-1.25	0.58-0.62	^{3}He	25	28	3425	49	3.5	
					^{3}H	25	27	3473	35	4.9	
					^{2}H	25	28	3433	51	7.4	**15.8/2**
2.200	26.2	1.770	0.84-1.20	0.77-0.83	^{3}He	25	7	3362	47	3.5	
					^{3}H	25	7	3284	34	4.9	
					^{2}H	25	7	3382	51	7.1	**15.5/2**
2.200	30.3	1.665	0.87-1.16	0.97-1.04	^{3}He	25	3	2352	30	3.5	
					^{3}H	25	2	3443	33	3.2	
					^{2}H	25	3	2376	34	6.7	**13.4/2**
								Total time needed (LEFT)			**379.6+22.4**

TABLE I: List of kinematics for the left HRS and estimated beam time needed for the proposed experiment. The last three settings will be measured with the left and right spectrometers running taking data simultaneously, so each requires only half of the full data taking time.

	^{3}He + ^{3}H + ^{2}H
Conf change	5 × 0.5 hr
Target motion	25 × 10 min
Beam energy change	8 hr
H-elastic	5 × 1 hr
Optics	5 × 0.5 hr
Dummy run	19 hr
BCM calibration	2 × 1 hr
Energy measurement	2 × 2 hr
Boiling study	8 hr
Rate-dependence tests	4 hr
Intial checkout	8 hr
TOTAL	48 hr

TABLE II: Summary of the overhead time.

E (GeV)	θ (deg)	E' (GeV)	x_{range}	Q^2_{range} (GeV/c)^2	Tg	I (μA)	psc	R_{tot} (Hz)	R_{phys} (Hz)	time (hrs)	Total (hrs)
4.400	24.5	3.100	0.90-1.14	2.37-2.54	^{3}He	25	1	593	8.7	7.0	
					^{3}H	25	1	584	7.1	8.9	
					^{2}H	25	1	607	11	11.1	**27.0**
4.400	24.5	2.890	0.73-0.90	2.21-2.37	^{3}He	25	1	1095	14	5.0	
					^{3}H	25	1	1084	31	5.7	
					^{2}H	25	1	1118	18	7.9	**18.6**
4.400	26.5	3.040	1.00-1.22	2.73-2.90	^{3}He	25	1	188	2.4	10.0	
					^{3}H	25	1	185	1.9	13.3	
					^{2}H	25	1	193	3.2	16.8	**40.1**
4.400	26.5	2.865	0.85-1.00	2.57-2.73	^{3}He	25	1	417	5.9	7.0	
					^{3}H	25	1	412	5.0	8.6	
					^{2}H	25	1	428	7.7	11.1	**26.7**
4.400	26.5	2.700	0.73-0.85	2.42-2.57	^{3}He	25	1	683	9.8	6.0	
					^{3}H	25	1	676	8.6	6.9	
					^{2}H	25	1	698	12	9.6	**22.6**
4.400	28.5	2.910	1.00-1.23	3.00-3.21	^{3}He	25	1	88	1.1	35.0	
					^{3}H	25	1	86	0.9	43.8	
					^{2}H	25	1	90	1.4	53.5	**132.3**
4.400	28.5	2.715	0.84-1.00	2.79-3.00	^{3}He	25	1	238	2.9	20.0	
					^{3}H	25	1	235	2.5	23.8	
					^{2}H	25	1	245	3.7	31.2	**75.0**
4.400	28.5	2.530	0.71-0.84	2.60-2.79	^{3}He	25	1	439	6.7	10.0	
					^{3}H	25	1	434	5.7	11.7	
					^{2}H	25	1	449	8.4	16.2	**38.0**
2.200	22.0	1.870	0.78-1.25	0.58-0.62	^{3}He	25	28	3425	49	3.5	
					^{3}H	25	27	3473	35	4.9	
					^{2}H	25	28	3433	51	7.4	**15.8/2**
2.200	26.2	1.770	0.84-1.20	0.77-0.83	^{3}He	25	7	3362	47	3.5	
					^{3}H	25	7	3284	34	4.9	
					^{2}H	25	7	3382	51	7.1	**15.5/2**
2.200	30.3	1.665	0.87-1.16	0.97-1.04	^{3}He	25	3	2352	30	3.5	
					^{3}H	25	2	3443	33	3.2	
					^{2}H	25	3	2376	34	6.7	**13.4/2**
								Total time needed (RIGHT)			**380.3+22.4**

TABLE III: List of kinematics for the right HRS and estimated beam time needed for the proposed experiment. The right HRS running is simultaneous to the left HRS running, and so does not increase the total time needed.

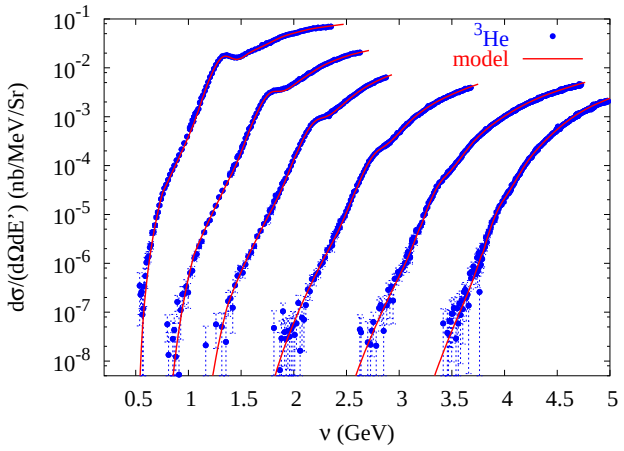

FIG. 17: Comparison of the XEM cross section model for ^{3}He with recent Hall C data [32]. These data cover a Q^2 range between approximatively 2 and 8 $(\mathrm{GeV/c})^2$ in the quasi-elastic region. The cross section spectrum at the lowest ν is in our proposed Q^2 range of 2 $(\mathrm{GeV/c})^2$.

Figure 17 shows a comparison of the model with the data from experiment E02-019 [33] from which the XEM model was generated. Figure 18 shows a comparison with existing world data on quasi-elastic scattering ^{3}He and ^{3}H [34] at lower Q^2. At these lower Q^2 values, the model is still in good agreement with the data from SLAC [35] and from MIT Bates Linear Accelerator Center [26]. While the model is fitted to the E02-019 kinematics (2–8 GeV^2 in the quasi-elastic region), it is good at approximately the 20% level down to Q^2 values below 0.5 GeV^2 based on a comparison to the database [34] and also at higher Q^2 values in the resonance region between 1.0 and 4.0 GeV^2 [30]. The projections used for the ^{3}He target in E08-014, covering a similar Q^2 range, demonstrate the accuracy of the model in this kinematic region.

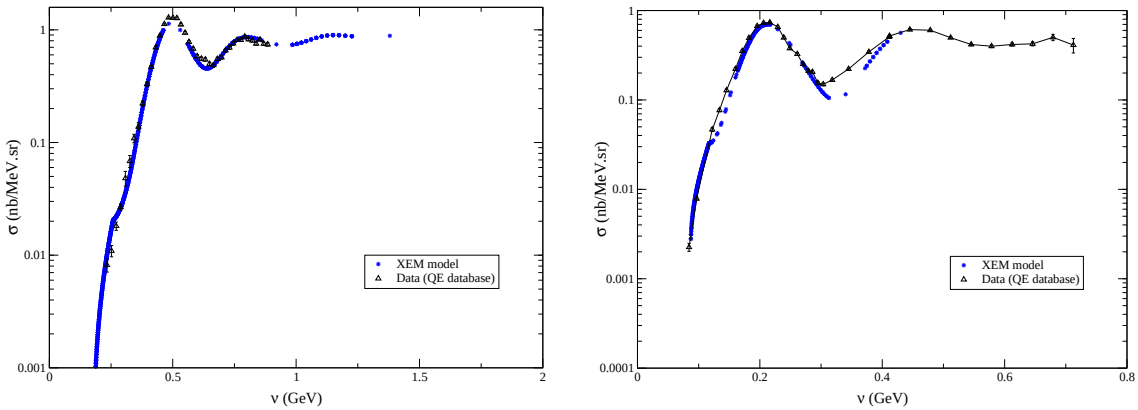

FIG. 18: Comparison of the XEM cross section model with world data [34]. Left plot: ^{3}He at incident energy 3.9 GeV and scattering angle 15° ($Q^2 \approx 0.9$ $(\mathrm{GeV/c})^2$). Right plot: ^{3}H at incident energy 0.79 GeV and scattering angle 54° ($Q^2 \approx 0.4$ $(\mathrm{GeV/c})^2$).

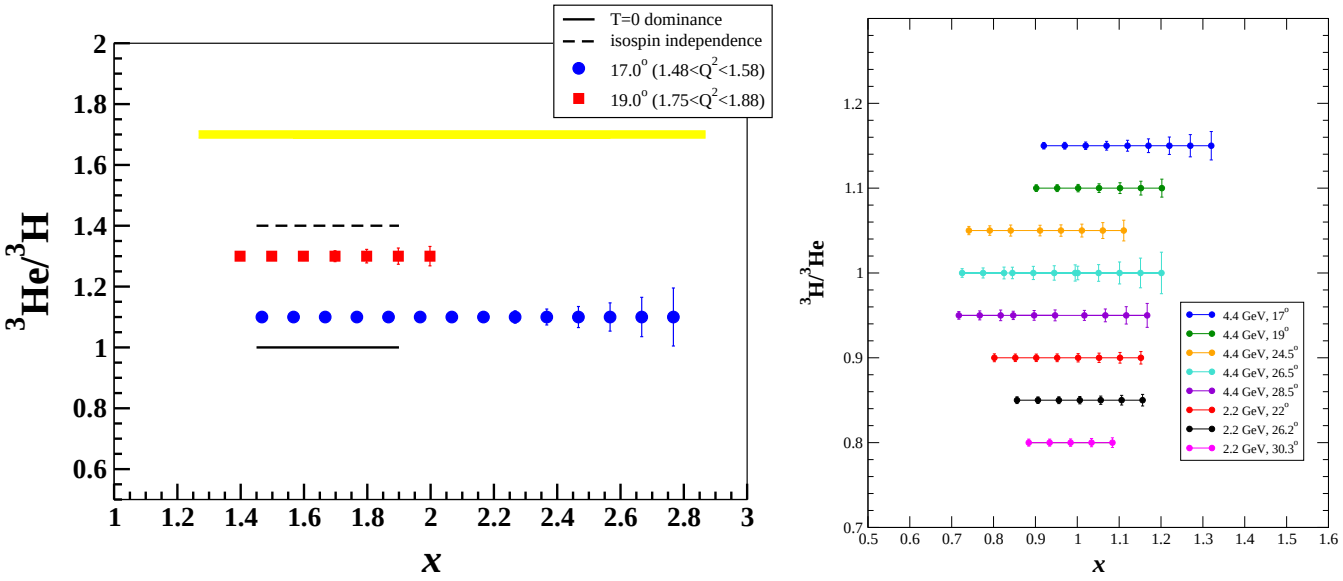

FIG. 19: **Left:** Projected statistical uncertainties for data taken at in the 2N-SRC and 3N-SRC region. The yellow bands represent a point-to-point systematic uncertainty of ±1.2%. The error band does not include the overall normalization uncertainty of 1.1%, dominated by the uncertainty in the relative target thicknesses. In the 2N-SRC region, the dashed line indicates the prediction for isospin-independent SRCs and the solid line represents isoscalar dominance. **Right:** The uncertainties for measurements in the quasi-elastic region; the systematic and normalization uncertainties are included in the error bars shown.

D. Projected results

The projected precision of our measurements in the 2N-SRC and 3N-SRC regions is shown in Fig. 19. Also drawn are the two cross section ratio predictions from the two isospin dependence assumptions. After combining of statistical and systematic uncertainties (see Table IV), it is clear that the sensitivity of our data will allow us to favor one or the other isospin dependence assumption of the pair in the 2N-SRC. Our expected total uncertainty in the 2N-SRC region is approximately 2%, which will provide a factor of 3-4 improvement of the isospin-dependence measurement compare to the results of Ref. [14]. In addition, we will pioneer the study of the isospin dependence of the 3N-SRCs with relatively precise data at $x > 2.2$. The solid and dashed lines in the left panel of Fig. 19 indicate the expected ratio in the 2N-SRC region for the limiting cases of isospin independence and isoscalar dominance. The limiting cases for the ^{3}He/^{3}H ratio, discussed in Sec. II D, yield to predictions for the ratio ^{3}He/^{3}H $\approx$ 0.35, 1.4, or 3.

The statistical projections of our proposed quasi-elastic scattering measurements on ^{3}He and ^{3}H are shown in Fig. 19. From the world data [34], the highest Q^2 reached in quasi-elastic scattering off ^{3}H is below 1.0 (GeV/c)^2. Our proposed measurements are at Q^2 between 1.4 and 2.7 (GeV/c)^2, which can be of great interest for few-body calculations.

E. Overhead time

The total overhead time needed for calibration, background study and configuration changes is provided below.

Calibration and background studies

We will need to measure the contributions from the aluminum entrance and exit windows of the target can. For each kinematic, 15% of the ^{3}He running time should be enough to accomplish a precise dummy subtraction. The time needed for dummy stainless-steel running is about 24 hours.

Two beam energy measurements (2 hrs each) and two BCM calibrations (1 hrs each) will be necessary. We will take optics data at each scattering angle. A 30 minute run on carbon foils for each angle will be sufficient.

We assume 8 hours for initial checkout. We plan to take elastic hydrogen data at each proposed scattering angle. An hour for each angle should be enough for a total of 5 hours (left and right HRSs running simultaneously).

Also we will conduct careful target boiling and rate dependence studies and ask for 12 hours of beamtime.

Configuration changes

We assume 30 minutes for a change of kinematic and 10 minutes for a target motion.

The total overhead for both parts of the experiment are summarized in Table II.

Systematic	$\delta\sigma/\sigma$	$\delta R/R$ (normalization)	$\delta R/R$ (pt-to-pt)
Acceptance correction	2.0%*	0.3%	1.0%
Radiative correction	3.0%*	0.4%	0.3%
Tracking efficiency	1.0%*	-	0.2%
Trigger efficiency	0.5%*	-	0.1%
PID efficiency	1.5%*	-	0.2%
Target thickness	1.0%†	1.0%	-
Charge measurement	0.5%	-	0.5%
Energy measurement	0.05%	-	-
COMBINED UNCERTAINTY	4.6%	1.1%	1.2%

TABLE IV: Relative systematic uncertainties in the extraction of the unpolarized cross sections from E01-012 [30] and of the cross section ratio from E03-103 [36]. Entries with an asterisk indicate corrections made directly on the cross section. Entries without asterisk indicate contributions to the overall uncertainty. For the target ratios, the acceptance correction is dominated by the target length acceptance, so a 0.3% relative uncertainty is estimated when taking the integrated yield ratio from two (identical) long targets. †We estimate a 2% uncertainty on the relative target thickness based on measurements of the target temperature and pressure, but can use the MARATHON low-x DIS data to acheive a 1% measurement of the relative normalization [28]).

IV. EXPERIMENTS WITH SIMILAR PHYSICS GOALS

This proposal is a logical follow-up of E08-014, which perform a Q^2-scan in the 2N and 3N-SRC in order to determine the onset of scaling and help in the establishment of more relevant scaling variables for the correlation region. Most directly related to this proposal, E08-014 also compared inclusive cross sections at $x > 1$ for ^{40}Ca and ^{48}Ca with the

goal of examining the isospin structure of 2N-SRCs. This is the main goal of the present proposal, and the use of ^{3}H and ^{3}He in this experiment provides two main improvements over the ^{40}Ca and ^{48}Ca comparison. First, nuclear structure calculations are more straightforward for the few-body nuclei, and structure differences should be smaller between ^{3}H and ^{3}He than ^{40}Ca and ^{48}Ca. Second, this proposal is more sensitive, with a 40% difference between the predictions of isospin-independent and isoscalar-dominated models compared to a 25% difference for the calcium isotopes. Finally, Oak Ridge provided the ^{48}Ca target but did not provide the requested ^{40}Ca target. Thus, the experiment was forced to run using a natural calcium target, and because it had to be made very quickly for the experiment, it has visible non-uniformities. The data was taken using a larger raster, and position scans were performed to determine how well the thickness can be extracted, but it is clear that the uncertainty in the relative thickness of the targets will be significantly larger than anticipated. A few-percent measurement of the difference in the calcium isotopes is still significant compared to the 25% difference in the predictions, but the proposed measurements will have $\sim$3 times the sensitivity with a 2% extraction (including normalization uncertainty) compared the 40% difference. In addition, the study of final-state interactions, the structure of 3N-SRCs, etc... go beyond the scope of the E08-014 proposal.

The isospin structure of the 2N-SRCs was first measured in two-nucleon knockout experiment E01-015 [14], and a recent extension of these measurements to higher missing momentum (E07-006) was just completed. The main advantage here is that we have much smaller contributions from final state interactions, allowing a clean and independent extraction of the isospin structure.

Experiment E12-06-105 is another inclusive study of SRCs, but does not focus on the isospin structure and is heavily weighted toward very large momentum transfers in an attempt to measure the quark distribution functions in nuclei.

While the main physics goals of the MARATHON proposal (E12-10-103) differ from our proposal, the main feature of both experiments is the use of the ^{3}H target. Both experiments will run using the same target configuration, and presumably both will run at the same time. Current discussions involve the target being put together in 2014 and 2015, and since the approved version of the MARATHON proposal uses only standard equipment (apart from the target), it could potentially be ready to run in 2015 or 2016. We assume that, if approved, we would run along with MARATHON, and thus could easily end up running within the first five years.

V. REQUEST TO THE LABORATORY

We are requesting 450 hours (about 19 days) of beam time which will be split into two running periods. The ^{3}He, ^{3}H and ^{2}H running will require 402 hours for the main data taking, 48 hours for configuration changes, calibration, checkout, and background runs. All times assume 100% running efficiency. To achieve our physics goal, we will use the same target design and setup as the fully approved 12 GeV experiment E12-10-103 [28]: 30cm ^{3}H, ^{3}He, ^{2}H, ^{1}H gas targets, an empty cell and the multi-foil optics targets. We will run with the HRS spectrometers using standard dectector packages.

VI. RESOURCES

The Medium Energy Physics group at Argonne National Laboratory has already declared commitment to part of the design and construction of the tritium target system for the fully approved experiment E12-10-103 [28].

The collaboration is also expected to make major contributions in the upgrade of Hall A beamline for various

approved 12 GeV proposals.

---

[1] L. Lapikas, Nucl. Phys. **A553**, 297c (1993).

[2] J. Arrington, D. Higinbotham, G. Rosner, and M. Sargsian (2011), arXiv:1104.1196.

[3] P. E. Ulmer et al., Phys. Rev. Lett. **89**, 062301 (2002).

[4] F. Benmokhtar et al. (Jefferson Lab Hall A), Phys. Rev. Lett. **94**, 082305 (2005).

[5] L. L. Frankfurt and M. I. Strikman, Nucl. Phys. **B181**, 22 (1981).

[6] L. L. Frankfurt and M. I. Strikman, Phys. Rept. **160**, 235 (1988).

[7] C. C. degli Atti and S. Simula, Phys. Lett. B **325**, 276 (1994).

[8] L. L. Frankfurt, M. I. Strikman, D. B. Day, and M. Sargsian, Phys. Rev. C **48**, 2451 (1993).

[9] K. S. Egiyan et al. (CLAS), Phys. Rev. Lett. **96**, 082501 (2006).

[10] K. S. Egiyan et al. (CLAS), Phys. Rev. C **68**, 014313 (2003).

[11] N. Fomin et al., to be submitted to PRL [copy submitted with proposal].

[12] J. Arrington et al., Phys. Rev. Lett. **82**, 2056 (1999).

[13] P. Solvignon, J. Arrington, D. B. Day, D. Higinbotham, et al., Jefferson Lab experiment E08-014.

[14] R. Shneor et al. (Jefferson Lab Hall A), Phys. Rev. Lett. **99**, 072501 (2007).

[15] R. Subedi et al., Science **320**, 1476 (2008).

[16] O. Benhar et al., Phys. Lett. B **343**, 47 (1995).

[17] M. M. Sargsian, Phys. Rev. **C82**, 014612 (2010), 0910.2016.

[18] M. M. Sargsian, private communication.

[19] L. Frankfurt, M. Sargsian, and M. Strikman, Int.J.Mod.Phys. **A23**, 2991 (2008).

[20] W. Bertozzi, E. Piasetzky, J. Watson, S. Wood, et al., Jefferson Lab experiment E01-015.

[21] R. Schiavilla, R. B. Wiringa, S. C. Pieper, and J. Carlson, Phys. Rev. Lett. **98**, 132501 (2007).

[22] M. M. Sargsian, T. V. Abrahamyan, M. I. Strikman, and L. L. Frankfurt, Phys. Rev. **C71**, 044615 (2005), nucl-th/0501018.

[23] S. C. Pieper and R. B. Wiringa, Ann. Rev. Nucl. Part. Sci. **51**, 53 (2001), nucl-th/0103005.

[24] R. B. Wiringa, private communication.

[25] M. I. Strikman, private communication.

[26] K. Dow et al., Phys. Rev. Lett. **61**, 1706 (1988).

[27] J. Lachniet et al. (CLAS), Phys. Rev. Lett. **102**, 192001 (2009), 0811.1716.

[28] G. Petratos, J. Gomez, R. Holt, R. D. Ransome, et al., Jefferson Lab proposal E12-10-103.

[29] **DOE HANDBOOK:** *tritium handling and safe storage* (March 2007), DOE-HDBK-1129-2007.

[30] P. Solvignon, Ph.D. thesis, Temple University (2006).

[31] J. Alcorn et al., Nucl. Inst. & Meth. **A522**, 294 (2004).

[32] N. Fomin, Ph.D. thesis, University of Virginia (2008).

[33] J. Arrington, D. Day, B. Filippone, A. F. Lung, et al., Jefferson Lab experiment E02-019.

[34] O. Benhar, D. Day, and I. Sick (2006), nucl-ex/0603029.

[35] Z. E. Meziani et al., Phys. Rev. Lett. **69**, 41 (1992).

[36] J. Seely, Ph.D. thesis, Massachusetts Institute of Technology (2006).

Draft of correlation paper from experiment E02-019 for PAC38

New measurements of high-momentum nucleons and short-range structures in nuclei.

N. Fomin,[1,2,3] J. Arrington,[4] R. Asaturyan,[5,*] F. Benmokhtar,[6] W. Boeglin,[7] B. Boillat,[8] P. Bosted,[9] A. Bruell,[9] M. H. S. Bukhari,[10] E. Chudakov,[9] B. Clasie,[11] S. H. Connell,[12] M. M. Dalton,[3] A. Daniel,[10] D. B. Day,[3] D. Dutta,[13,14] R. Ent,[9] L. El Fassi,[4] H. Fenker,[9] B. W. Filippone,[15] K. Garrow,[16] D. Gaskell,[9] C. Hill,[3] R. J. Holt,[4] T. Horn,[6,9] M. K. Jones,[9] J. Jourdan,[8] N. Kalantarians,[10] C. E. Keppel,[9,17] D. Kiselev,[8] M. Kotulla,[8] K. Kramer,[14] R. Lindgren,[3] A. F. Lung,[9] S. Malace,[17] P. Markowitz,[7] P. McKee,[3] D. G. Meekins,[9] T. Miyoshi,[18] H. Mkrtchyan,[5] T. Navasardyan,[5] G. Niculescu,[19] Y. Okayasu,[18] A. K. Opper,[20] C. Perdrisat,[21] D. H. Potterveld,[4] V. Punjabi,[22] X. Qian,[14] P. E. Reimer,[4] J. Roche,[20,9] V.M. Rodriguez,[10] O. Rondon,[3] E. Schulte,[4] J. Seely,[11] E. Segbefia,[17] K. Slifer,[3] G. R. Smith,[9] P. Solvignon,[9] V. Tadevosyan,[5] S. Tajima,[3] L. Tang,[9,17] G. Testa,[8] R. Trojer,[8] V. Tvaskis,[17] W. F. Vulcan,[9] C. Wasko,[3] F. R. Wesselmann,[22] S. A. Wood,[9] J. Wright,[3] and X. Zheng[3,4]

[1] *Los Alamos National Laboratory, Los Alamos, NM, USA*
[2] *University of Tennessee, Knoxville, TN, USA*
[3] *University of Virginia, Charlottesville, VA, USA*
[4] *Physics Division, Argonne National Laboratory, Argonne, IL, USA*
[5] *Alikhanyan National Scientific Laboratory, Yerevan 0036, Armenia*
[6] *University of Maryland, College Park, MD, USA*
[7] *Florida International University, Miami, FL, USA*
[8] *Basel University, Basel, Switzerland*
[9] *Thomas Jefferson National Laboratory, Newport News, VA, USA*
[10] *University of Houston, Houston, TX, USA*
[11] *Massachusetts Institute of Technology, Cambridge, MA, USA*
[12] *University of Johannesburg, Johannesburg, South Africa*
[13] *Mississippi State University, Mississippi State, MS, USA*
[14] *Duke University, Durham, NC, USA*
[15] *Kellogg Radiation Laboratory, California Institute of Technology, Pasadena, CA, USA*
[16] *TRIUMF, Vancouver, British Columbia, Canada*
[17] *Hampton University, Hampton, VA, USA*
[18] *Tohoku University, Sendai, Japan*
[19] *James Madison University, Harrisonburg, VA, USA*
[20] *Ohio University, Athens, OH, USA*
[21] *College of William and Mary, Williamsburg, VA, USA*
[22] *Norfolk State University, Norfolk, VA, USA*

(Dated: July 5, 2011)

We present new, high-Q^2 measurements of inclusive scattering from high-momentum nucleons in nuclei. This yields an improved extraction of the strength of two-nucleon correlations for several nuclei, including light nuclei where clustering effects can, for the first time, be examined. The data extend to the kinematic regime where three-nucleon correlations are expected to dominate and we observe significantly greater strength in this region than previous measurements.

PACS numbers:

Obtaining a complete understanding of the complex structure of nuclei is one of the major goals of nuclear physics. Significant progress has been made over the past decade, and there now exist several *ab initio* approaches to calculating the structure of light nuclei based on the nucleon-nucleon (and three-nucleon) interactions, as well as approaches that extend to heavier nuclei. One of the least understood aspects of nuclei is their short-range structure, where nucleons are close together and interact via the poorly-constrained short-range repulsive core of the N–N interaction. This generates configurations where two nucleons have large, nearly back-to-back momenta within the nucleus, providing access to the short-range structure of nuclei through measurements of scattering from high-momentum nucleons [1–3].

Experimentally, one can access this regime through inclusive quasielastic scattering, in which a virtual photon of energy ν and momentum $\vec{q}$ is absorbed on a single nucleon. Elastic scattering from a nucleon at rest yields well defined scattering kinematics, corresponding to $x \equiv Q^2/2M\nu = 1$, where M is the nucleon mass and $Q^2 = q^2 - \nu^2$. For quasielastic scattering from a nucleon moving in the nucleus, this distribution is broadened and the cross section is peaked around $x = 1$, with a width characterized by the Fermi momentum and tails that extend to higher momentum arising from hard interactions

of two or more nucleons. Inclusive scattering at high Q^2 minimizes final-state interactions, while low energy transfer, ν, suppresses inelastic contributions. Thus, inclusive scattering at large Q^2 on the low energy loss side of the quasielastic peak, corresponding to $x > 1$, allows for relatively clean isolation of quasielastic scattering from high-momentum nucleons. We present new measurements of inclusive scattering from very high-momentum nucleons in the deuteron as well as a range of light and heavy nuclei. These measurements provide a probe of the high-momentum, short-distance structure in nuclei.

Experiment E02-019 was performed in Hall C at the Thomas Jefferson National Accelerator Facility (JLab). A continuous wave electron beam of 5.766 GeV at currents of up to 80 μA impinged on targets of ^{2}H, ^{3}He, ^{4}He, Be, C, Cu, and Au. Scattered electrons were detected using the High Momentum Spectrometer (HMS) for $\theta = 18°$, $22°$, $26°$, $32°$, $40°$, and $50°$. A detailed description of the measurement and the analysis is available in Refs. [4, 5].

Most of the dominant systematic uncertainties are discussed in Ref. [4], but for the low Q^2 and large x kinematics relevant to this analysis, some corrections become more significant. For the cryogenic targets, contributions from scattering in the aluminum endcaps of the target must be subtracted. At large x values, this contribution becomes significant, especially for the ^{3}He target, where endcap scattering yields up to 40% (60%) of the cross section for $x > 1.5$ ($x > 2$). We measured scattering from an aluminum "dummy" target in order to remove the endcap contribution. Because the radiative corrections are large for $x > 1$, we include a correction to account for the difference between the radiative corrections in the dummy target and the cryogenic targets. The increased thickness of the dummy target can yield a radiative correction factor that differs from the hydrogen target by up to 10%. We apply a systematic uncertainty equal to 3% of the subtraction to account for uncertainties in the relative contribution from the endcaps and the dummy target. The cross sections were corrected for Coulomb effects using the prescription of Ref. [6]. The correction is small for light nuclei, but can be as large as 5% (10%) for copper (gold). We include a systematic uncertainty equal to 20% of the calculated correction. The uncertainty due to possible offsets in the beam energy or spectrometer kinematics is $\lesssim$5% in the cross sections for $x < 2$, but $\lesssim$2% in the target ratios.

Traditionally, inclusive cross sections at $x > 1$ have been analyzed in the context of y-scaling [1, 3]. In this approach, the high-Q^2 quasielastic cross section reduces to a product of the e–N elastic cross section, σ_{eN}, and a scaling function, $F(y, Q^2)$. If the y-scaling approximations are valid, y is the initial longitudinal momentum of the struck nucleon, $F(y, Q^2)$ will depend only on y at large Q^2 values, and in this limit, $F(y)$ will be directly related to the nucleon momentum distribution. In the most straightforward y-scaling analysis, y is determined from energy conservation, assuming that the final state consists of the struck nucleon and the unexcited (A-1) spectator nucleus:

$$\nu + M_A = (M_N^2 + (q+y)^2)^{\frac{1}{2}} + (M_{A-1}^2 + y^2)^{\frac{1}{2}} \ , \quad (1)$$

where M_N is the mass of the struck nucleon, M_A and M_{A-1} are the masses of the target and spectator (A-1) nuclei. The scaling function $F(y)$ is extracted from the measured cross section [1, 3]:

$$F(y) = \frac{d^2\sigma}{d\Omega d\nu}[Z\sigma_p + N\sigma_n]^{-1} \frac{q}{(M^2 + (y+q)^2)^{\frac{1}{2}}} \ . \quad (2)$$

If the above assumptions are valid and final state interactions are negligible, one can extract the nucleon momentum distribution, $n(k)$:

$$n(k) = \frac{-1}{2\pi k} \frac{dF(k)}{dk} \ . \quad (3)$$

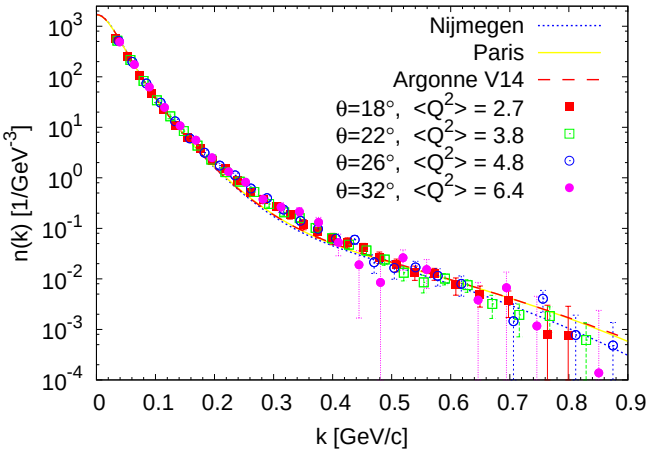

FIG. 1: (Color online) The deuteron momentum distribution extracted from the E02-019 data along with $n(k)$ calculated using three different N–N potentials. Note that the Paris and Av14 calculations are nearly indistinguishable on this scale.

Figure 1 shows the momentum distribution extracted from the new E02-019 data on deuterium, along with calculations based on three N–N potentials. The lack of Q^2 dependence and general agreement with the calculations at large k suggests that the final state interaction contributions here are not large, although it is hard to set quantitative limits because the N–N potential is not well constrained at large momenta. The excess in the extracted momentum distribution at $k \approx 0.3$ GeV/c is a common feature of previous extractions from both inclusive and D(e,e'p) extractions [3, 7].

ANYTHING MORE TO SAY ABOUT $k \approx 0.3$*???*.

While this approach appears to be very successful for the deuteron, the assumption of an unexcited spectator in Eq. 1 breaks down for heavier nuclei. In the deuteron,

it takes significant energy to exceit the spectator nucleon, while for heavier nuclei, the (A-1) spectator can break up or have low energy nuclear excitations. In fact, the idea that the nucleus has pairs of high-momentum, back-to-back nucleons coming from short-range interactions suggests that even in the pure spectator picture, striking one of these high momentum nucleons will leave the spectator system in an excited state of one fast nucleon and an (A-2) system nearly at rest. Several attempts have been made to account for this, either with a Q^2-dependent binding correction to $F(y)$ or a modified scaling variable that accounts for the high-momentum spectators at large values of k [1, 8]. These approaches provide improved but model-dependent extractions of the momentum distribution. To avoid this model dependence, one can make direct comparisons of the heavier nuclei to deuterium at large x, where scattering from nucleons below the Fermi momentum is forbidden. If these high-momentum components are related to two-nucleon correlations (2N-SRCs), then they should yield the same high-momentum tail whether in a heavy nucleus or a deuteron.

The first detailed study of SRCs in inclusive scattering combined data from several measurements at SLAC [9], so the cross sections had to be interpolated to identical kinematics to form the ratios. A plateau was seen in the ratio $(\sigma_A/\mathrm{A})/(\sigma_D/2)$ that was roughly A-independent for $\mathrm{A} \geq 12$, but smaller for ^{3}He and ^{4}He. Ratios from Hall B at JLab showed similar plateaus [10, 11] and mapped out the Q^2 dependence at low Q^2, seeing a clear breakdown of the picture for $Q^2 < 1.4$ GeV^2. However, these measurements did not include deuterium; only A/^{3}He ratios were available. Finally, JLab Hall C data at 4 GeV [12, 13] measured scattering from nuclei and deuterium at larger Q^2 values than the previous measurements, but the deuterium cross sections had limited x coverage. Thus, while there is significant evidence for the presence of SRCs in inclusive scattering, clean and precise ratio measurements for a range of nuclei are lacking.

Figure 2 shows the A/D cross section ratios for the E02-019 data at a scattering angle of 18°. For $x > 1.5$, the data show the expected near-constant behavior, although the point at $x = 1.95$ is always high because the ^{2}H cross section approaches zero as $x \to M_D/M_p \approx 2$. This was not observed before, as the previous SLAC ratios had much wider x bins and larger statistical uncertainties, while the CLAS took ratios to ^{3}He.

Table I shows the ratio in the plateau region for a range of nuclei at all Q^2 values where there was sufficient large-x data. We apply a cut in x to isolate the plateau region, although the onset of scaling in x varies somewhat with Q^2. The start of the plateau corresponds to a fixed value of the light-cone momentum fraction of the struck nucleon, α_i [1, 9]. However, α_i requires knowledge of the initial energy and momentum of the struck nucleon, and so is not directly measured in inclusive scattering. Thus, the plateau region is typically examined as a function of

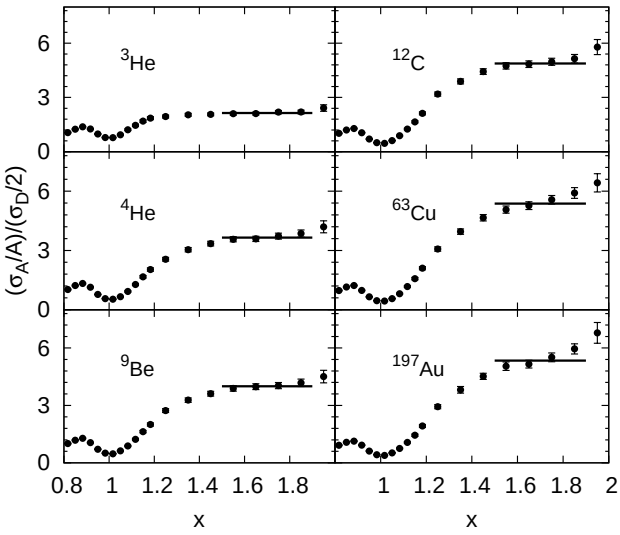

FIG. 2: Per-nucleon cross section ratios vs x at θ=18°.

x or α_{2n}, which corresponds to α_i under the approximation that the photon is absorbed by a single nucleon from a pair of nucleons with zero net momentum [9]. We take the A/D ratio for $x_{min} < x < 1.9$, such that the x_{min} value corresponds to a fixed value of α_{2n}. The upper limit is included to avoid the deuteron kinematic threshold.

TABLE I: $r(A,D) = (2/A)\sigma_A/\sigma_D$ in the 2N correlation region ($x_{min} < x < 1.9$). The value of x_{min} is chosen to keep the minimum value of α_{2n} fixed at 1.275. The last column is the ratio at 18° after the subtraction of the estimated inelastic contribution (with a systematic uncertainty of 100% of the subtraction).

A	θ=18°	θ=22°	θ=26°	Inel.sub
^{3}He	2.14±0.04	2.28±0.06	2.33±0.10	2.13±0.04
^{4}He	3.66±0.07	3.94±0.09	3.89±0.13	3.60±0.10
Be	4.00±0.08	4.21±0.09	4.28±0.14	3.91±0.12
C	4.88±0.10	5.28±0.12	5.14±0.17	4.75±0.16
Cu	5.37±0.11	5.79±0.13	5.71±0.19	5.21±0.20
Au	5.34±0.11	5.70±0.14	5.76±0.20	5.16±0.22
$\langle Q^2 \rangle$	2.7 GeV^2	3.8 GeV^2	4.8 GeV^2	
x_{min}	1.5	1.45	1.4	

There is a systematic 5–7% difference between the lowest Q^2 data set and the higher Q^2 values. At these high Q^2 values, there is some inelastic contribution to the cross section, even at these large x values. While this is approximately a 1–3% contribution at 18°, based on our model of the cross section, it can be 5–10% at the larger angles, and explains much of the observed Q^2 dependence. Thus, we use only the 18° data, corrected for our estimated inelastic contribution, in extracting the contribution of SRCs.

The typical assumption for this kinematic regime is that the FSIs in the high-x region come only from rescattering between the nucleons in the initial-state correla-

tion, and so the FSIs cancel out in taking the ratios [1–3, 9]. However, it has been argued that while the ratios are a signature of SRCs, they cannot be used to provide a quantitative measurement since different targets may have different FSIs [14]. With the higher Q^2 reach of these data, there is relatively little Q^2 dependence, supporting the assumption of cancellation of FSIs in the ratios. Updated calculations for both deuterium and heavier nuclei are underway to further examine the question of FSI contributions to the ratios [15].

Assuming that the high-momentum contribution comes entirely from quasielastic scattering from a nucleon in an n–p SRC at rest, the cross section ratio σ_A/σ_D yields the number of nucleons in high-relative momentum pairs relative to the deuteron and $r(A,D)$ represents the relative probability for a nucleon in nucleus A to be in such a configuration. To extract the relative contribution of 2N-SRCs, we must use the inelastic-subtracted ratios and apply a correction for the smearing effect of the center-of-mass motion of the 2N-SRC pairs. The momentum distribution of a nucleon in the 2N-SRC will be a convolution of the relative distribution and the CM motion of the pair, as discussed (and extracted for Carbon) in Ref. [16]. This smearing of the distribution enhances the high-momentum tails in heavy nuclei, estimated to be a 20% correction for Fe [17]. Thus, for iron we would reduce the measured cross section ratio by a factor of 1.2 and scale the correction to the other nuclei based on an estimate of the pair motion as a function of A. We apply an uncertainty equal to 30% of this correction (50% for ^{3}He). In addition to enhancing the high-momentum tails, this effect can also yield some distortion in the shape at the largest x values. This may explain the small x dependence in the ratios in Fig. 2, which is larger for the heavy nuclei.

TABLE II: Extracted value of $R_{2N}(A)$. The results from SLAC [9] and CLAS [11] have been updated to be consistent with the new extraction except for the lack of Coulomb correction or inelastic subtraction (see text for details).

A	R_{2N} (E02-019)	SLAC	CLAS	CM corr
^{3}He	1.93±0.10	1.8±0.3	–	1.10±0.05
^{4}He	3.02±0.17	2.8±0.4	2.80±0.28	1.19±0.06
Be	3.37±0.17	–	–	1.16±0.05
C	4.00±0.24	4.2±0.5	3.50±0.35	1.19±0.06
Cu(Fe)	4.33±0.28	(4.3±0.8)	(3.90±0.37)	1.20±0.06
Au	4.26±0.29	4.0±0.6	–	1.21±0.06
$\langle Q^2 \rangle$	~2.7 GeV^2	~1.2 GeV^2	~2 GeV^2	
x_{min}	1.5	–	1.5	
α_{min}	1.275	1.25	1.22–1.26	

After correcting the measured ratios for the inelastic contribution and the enhancement of the high-momentum tails due to motion of the pair, we obtain R_{2N}, given in Tab. II, which represents the probabilty of a nucleon in nucleus A to be in a high relative momentum pair compared to a nucleon in the deuteron. It also shows updated extractions from previous measurements, with the C.M. motion correction applied to all experiments, and with the "isoscalar" correction factor removed from the previous works. This correction was based on the assumption that the high-momentum tails would have greater neutron contributions for N>Z nuclei. However, the dominance of isosinglet pairs [16, 18, 19] suggests that the high-momentum tail will have equal contributions from protons and neutrons. After making consistent extractions from all of the experiments, we find a systematic difference between our data and the CLAS results. While the CLAS data are closer to our Q^2 value than the SLAC data, their cut of $x > 1.5$ corresponds to lower minimum value α_{2n}, and if α_{2n} is not high enough to fully isolate 2N-SRCs, one expects the extracted ratio to be smaller. Our results have smaller uncertainties and a more conservative α_{min} cut, providing a cleaner extraction of the SRC contributions. Note that the previous experiments do not include any corrections (or uncertainties) associated with inelastic contributions or Coulomb distortion, the latter of which is estimated to be up to 6% for the Fe data of Ref. [11], and similar or larger for the lower Q^2 SLAC data [9].

Previous extractions of the strength of 2N-SRCs found a slow increase of R_{2N} with A in very light nuclei, with little apparent A dependence for A>12. The additional corrections applied in our extraction of 2N-SRC contributions do not modify these basic conclusions, but these corrections, along with the improved precision in our extraction yields a more detailed picture of the A dependence. In a mean-field model, one would expect the probability for two nucleons to be close enough together to form an SRC to be proportional to the average density of the nucleus [2]. However, while the density of ^{9}Be is well below that of ^{4}He or ^{12}C, and very similar to that of ^{3}He, the relative contribution from SRCs in ^{9}Be is much closer to that in ^{4}He or ^{12}C, suggesting that the simple expectation that SRCs will scale with density is insufficient. This is very much like the recently observed A dependence of the EMC effect [20], which also observed that ^{9}Be behaved more like denser nuclei due to the significant cluster structure in ^{9}Be. It seems clear that cluster structure should be extremely important in examining the short-range structure and contribution of SRCs in nuclei, but it has not been observed before, as previously-measured nuclei did not have sufficient clustering to yield a deviation from a simple scaling with density [11].

If one examines ratios to ^{3}He above $x = 2$, one expects the contribution from two-nucleon configurations to become small and eventually 3N-SRCs should dominate. The $x > 2$ region was examined in the CLAS analysis [11], but the statistics did not allow for an examination of the onset of scaling at high Q^2. They assumed that $Q^2 = 1.4$ GeV^2 would be sufficient to cleanly isolate 3N-

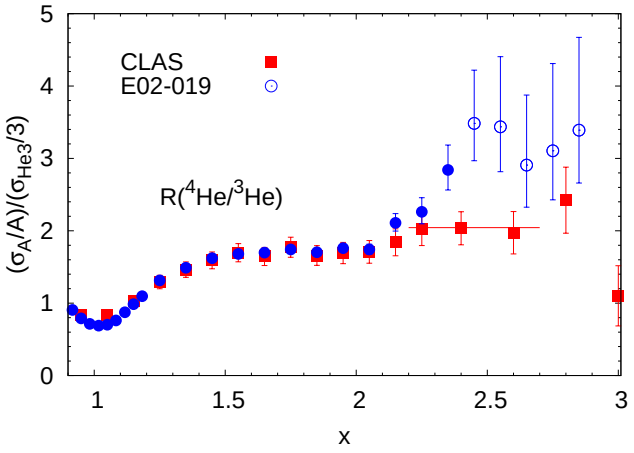

FIG. 3: (Color online) The ^{4}He/^{3}He ratios from CLAS and E02-019 (18° data). Errors shown are the combined statistical and systematic uncertainties. The error bars shown for $x \geq 2.4$ (hollow points) represent the central 68% confidence level region.

SRCs, but it is not clear that this is high enough. Choosing a minimum x and Q^2 value yields a minimum struck nucleon momentum. Near the Fermi momentum, the single particle contributions to $n(k)$ fall off rapidly, while the 2N-SRC contributions extend much further. Thus, choosing k_{min} somewhat above k_{Fermi} cleanly isolates the 2N-SRC contributions. While the 3N-SRC contributions should eventually dominate, the 2N and 3N-SRC contributions to $n(k)$ are more similar, and it may be a more gradual transition from 2N- to 3N-SRC dominance and it is not clear what kinematic cuts will cleanly isolate the 3N contributions.

Figure 3 shows the ^{4}He/^{3}He cross section ratio, along with the same ratios from CLAS [11] (leaving out their isoscalar correction). The ratios in the 2N-SRC region are in good agreement, while the difference near $x = 1$ is related to the lower resolution of the CLAS data, yielding a broader quasielastic peak for ^{3}He. However, even with the large uncertainties above $x = 2$, it is clear that the ratio at $x > 2.25$ is significantly higher at our Q^2 value (≈ 2.9 GeV^2), suggesting that the CLAS measurement ($\langle Q^2 \rangle \approx 1.6$ GeV^2) was not at sufficient Q^2 to able to cleanly isolate the contributions from 3N-SRCs.

In summary, we present new, high Q^2 measurements of scattering from high momentum nucleons in a range of nuclei. With these data, we have examined the high-momentum tails of the deuteron momentum distribution and used target ratios at $x > 1$ to examine the A and Q^2 dependence of the contribution of 2N-SRCs. The contribution from the 2N-SRCs is extracted with improved statistical and systematic uncertainties and with corrections for the previously ignored isoscalar dominance and motion of the pair in the nucleus. The ^{9}Be data show a significant deviation from predictions that the 2N-SRC contribution should scale with density, presumably due to strong clustering effects. At $x > 2$, where 3N-SRCs are expected to dominate, our A/^{3}He ratios are significantly higher than previous measurements at lower Q^2, suggesting that the scaling regime was not reached in previous measurements, and that the contributions from 3N-SRCs in heavy nuclei is larger than previously believed. A recently completed experiment [21] will map out x and Q^2 dependence in the 3N-SRC region with high precision, providing a definitive answer and will also compare ^{40}Ca and ^{48}Ca to provide a further test of the assumption of isoscalar dominance in the 2N-SRCs.

We thank the JLab technical staff and accelerator division for their contributions. This work supported in part by the NSF and DOE, including DOE contract DE-AC05-06OR23177 under which JSA, LLC operates JLab, and the South African NRF.

* Deceased
[1] J. Arrington, D. Higinbotham, G. Rosner, and M. Sargsian (2011), arXiv:1104.1196.
[2] L. L. Frankfurt and M. I. Strikman, Phys. Rept. **76**, 215 (1981).
[3] D. B. Day, J. S. McCarthy, T. W. Donnelly, and I. Sick, Ann. Rev. Nucl. Part. Sci. **40**, 357 (1990).
[4] N. Fomin et al., Phys.Rev.Lett. **105**, 212502 (2010).
[5] N. Fomin, Ph.D. thesis, University of Virginia (2007), arXiv:0812.2144.
[6] A. Aste, C. von Arx, and D. Trautmann, Eur. Phys. J. **A26**, 167 (2005).
[7] A. Bussiere, J. Mougey, D. Royer, D. Tarnowski, S. Turck-Chieze, et al., Nucl.Phys. **A365**, 349 (1981).
[8] C. Ciofi degli Atti and C. B. Mezzetti, Phys. Rev. **C79**, 051302 (2009), 0904.0443.
[9] L. L. Frankfurt, M. I. Strikman, D. B. Day, and M. Sargsian, Phys. Rev. C **48**, 2451 (1993).
[10] K. S. Egiyan et al., Phys. Rev. C **68**, 014313 (2003).
[11] K. S. Egiyan et al. (CLAS), Phys. Rev. Lett. **96**, 082501 (2006).
[12] J. Arrington et al., Phys. Rev. Lett. **82**, 2056 (1999).
[13] J. Arrington et al., Phys. Rev. C **64**, 014602 (2001).
[14] O. Benhar et al., Phys. Lett. B **343**, 47 (1995).
[15] O. Benhar, private communication.
[16] R. Subedi et al., Science **320**, 1476 (2008), 0908.1514.
[17] C. C. degli Atti and S. Simula, Phys. Rev. C **53**, 1689 (1996).
[18] M. M. Sargsian, T. V. Abrahamyan, M. I. Strikman, and L. L. Frankfurt, Phys. Rev. **C71**, 044615 (2005).
[19] R. Schiavilla, R. B. Wiringa, S. C. Pieper, and J. Carlson, Phys. Rev. Lett. **98**, 132501 (2007).
[20] J. Seely et al., Phys. Rev. Lett. **103**, 202301 (2009).
[21] J. Arrington, D. Day, D. W. Higinbotham, P. Solvignon, et al., Jefferson Lab Experiment E08-014 (2008).